Analysis of CO_2/CH_4 gas permeation of gamma-cyclodextrin based polymeric mixed matrix membrane

By

Ovaid Mehmood

School of Chemical and Materials Engineering (SCME)

National University of Science and Technology (NUST)

2019

Analysis of CO_2/CH_4 gas permeation of gamma-cyclodextrin based polymeric mixed matrix membrane

Name: Ovaid Mehmood

Reg. No: 00000171465

This thesis is submitted as a partial fulfillment of the requirements for the degree of

MS in Chemical Engineering

Supervisor Name: Dr. Sarah Farrukh

School of Chemical and Materials Engineering (SCME)

National University of Sciences and Technology (NUST)

H-12 Islamabad, Pakistan

April, 2019

Dedication

I dedicate this work to my parents, whose unwavering support and confidence in my abilities has made this work much easier

Acknowledgment

All praise belongs to Allah Almighty, the Most Benevolent, the Most Merciful, who has granted me the strength, courage and willpower to complete my work, and to overcome all the impediments that come in my way. I consider myself, highly fortunate to be able to complete this work in the time allotted to me.

My utmost gratitude to my supervisor, Dr. Sarah Farrukh, for her immense and unflinching support for completing my work. I am thankful to her for always believing in my abilities, and always being there for my assistance.

I owe a huge debt of gratitude to my Guidance and Examination Committee (GEC) members, Dr. Arshad Hussain and Dr. Erum Pervaiz, for their advice in easing the difficulties and removing many problems in my project. I am also thankful to them for their moral as well as material assistance.

I would also like to thank the lab staff for their help in carrying out the required testing and characterization techniques. I am thankful, especially to Dr. Sajid Iqbal from IST, Islamabad for their invaluable help in SEM spectroscopy. I am grateful for Comsats University Lahore for their cooperation in GC testing.

Finally, I am immensely gratified to my family and friends, who have been the source of endless support and encouragement for me, especially when I was in troubled waters regarding my project. They have given me much needed moral support, to complete my work.

Abstract

In today's world, energy crisis is a prevalent problem and to overcome this, carbon dioxide must be separated from fuel gases to improve the energy content of the fuel. This can be achieved by employing either conventional or un-conventional processes. In this thesis, separation is being done by using polymeric membranes and better results were achieved in terms of permeability and selectivity of CO_2 and CH_4. For this purpose, it is proposed to use mixed matrix membrane, which consists of Gamma-cyclodextrin-metal organic frame work (γ-CD-MOF) incorporated into two polymers mainly: polyurethane and cellulose acetate. γ-CD-MOF is classified under the category of green mof synthesized from potassium hydroxide (KOH) and cyclodextrin from starch by employing vapor-diffusion method. Having body centered cubic structure with cavity diameter 7.8A and spherical voids of 17A. γ-CD-MOF gained significant attention for being used as gas adsorbent material. Therefore, it is recommended to be used as filler in polymeric membrane for fabrication of mixed matrix membrane. Hence, CA/ γ-CD-MOF and PU/γ-CD-MOF mixed matrix membrane were synthesized from solution casting method and characterized by using SEM analysis, FTIR spectroscopy, XRD analysis and ultimate tensile testing In this thesis γ-CD-MOF is being incorporated into cellulose acetate and polyurethane and fabricate. These membranes undergo different characterization techniques i.e. SEM analysis, FTIR, XRD and ultimate tensile testing. These two membranes were then tested for gas permeation using single and mixed gas permeation testing of carbon dioxide and methane using gas chromatogram. It was found that CA/γ-CD-MOF membrane gave CO_2/CH_4 selectivity up to 39 but with low permeability of CO_2. While, CO_2/CH_4 selectivity achieved up to 29 and permeability maximum of 214 barrer of CO_2 in PU/γ-CD-MOF membranes. Both membranes possess highly dense surface morphology and no voids or cavities have been seen even at magnification of 20000x in SEM images. These features endorse solution-diffusion mechanism for the transport of gases through these dense membranes. After studying these two types of membranes, it was concluded that CA/γ-CD-MOF membrane employed where only focus in on high selectivity of carbon dioxide. To achieve better selectivity along with high permeability of carbon dioxide PU/γ-CD-MOF membrane is most suitable candidates for gas separation.

Table of contents

List of tables

List of figures

List of acronym

Γ-CD-MOF	gamma-cyclodextrin-metal organic frame work
PU	polyurethane
CA	cellulose acetate
SEM	Scanning Electron Microscopy
FTIR	Fourier Transform Infra-red (Spectroscopy)
XRD	x-ray diffraction
GC	gas chromatography
MMM	mixed matrix membrane
UTM	ultimate tensile machine
HKUST-1	Hong Kong university of science and technology-1
ZIF-8	Zeolitic imidazole frame work
MIL-53	Material Institute Lavoisier
KOH	potassium hydroxide
THF	tetra hydro furan
MWCNT	multi-walled carbon nano tubes
PEG	polyethylene glycol

Chapter 1

Introduction

1.1Background

In 2018 global carbon dioxide emission reached an all-time high since industrial revolution. Global carbon project estimates that 2.7 percent rise occurred in carbon dioxide concentration in atmosphere only in 2018 compared to last three years statistical data. Fossil fuel related carbon dioxide emission hit 37.1 billion metric ton in 2018. This rise in CO_2 emission also increase temperature globally $1.5C^0$ that cause massive melting of glaciers and rise in sea level and also caused damage to life and property [1]. Natural gas also contains significant concentration of CO_2 in addition to H_2S, N_2 and water vapors. Some other sources of CO_2 are biogas from anaerobic processes, flue gases from combustion of coal and fossil fuel and also from partial oxidation of certain organic compounds. In natural gas the presence of CO_2 and other acidic gases decrease the calorific value of methane and increase corrosiveness of gas stream that induce corrosion in distribution lines. Its compulsory to keep the concentration of CO_2 below 2% in natural gas stream for distribution[2]. So it is necessary to separate CO_2 from various gas streams including: sweetening of natural gas, separation of CO_2 and other impurities from biogas[3]. Consequently CO_2 separated from these sources is highly concentrated form and it can be stored in deep underground reserves by the process called carbon sequestration and also used for enhanced oil recovery purpose in oil and gas wells [3].

Our focus in this work is to separate CO_2 from natural gas, to boost the calorific value of fuel as stated earlier. Natural gas is a major source of energy for both industries and household use. The major combustible portion of natural gas is methane with a considerable amount of ethane and propane. Other than the major components, natural gas also contains a substantial amount of impurities, including acidic gases mainly H_2S, SO_2, CO and CO_2. As mentioned earlier, population has drastically increased, and this increased population requires increased energy output, which in turn requires increased fuel resources as our current fuel resources are already depleting very fast. So, the only solution is to improve the energy acquired from fuel gases. We have already seen that,

increasing the amount of CO2 reduces the energy output of fuel gases, so if we are to increase the output from conventional energy resources, we must lessen the concentration of carbon dioxide in the natural gas being used.

For the purpose of CO2 separation from various gases, including natural gas, we have a number of techniques, namely gas absorption through liquids, gas adsorption on solid surfaces, and membrane gas separation. Liquid gas absorption and adsorption on solid surfaces are two techniques which have been most developed, and are considered most suitable for CO2 separation. Both these processes are widely used in the industry for gas separation. However, there are several drawbacks of these two techniques, and the main drawback is that both these techniques are energy-intensive. This means that the amount of energy acquired from natural gas by reducing its carbon dioxide content is offset by the extra amount of energy used up in removing or capturing the said carbon dioxide gas.

Therefore, a less energy-intensive and a more energy-efficient process is required for CO2 separation, and research has been underway to find such a process or technique. Several decades of research have found that the most suitable process which fulfils these criteria is membrane gas separation, as it uses much less energy than conventional gas separation techniques. Membrane processes use about 40-50% of the energy used by these thermally demanding techniques. Also, membranes are a very promising technique to replace the conventional separation methods, because of their ease of manufacture, ease of integration into the existing industries and ease of scale-up.

1.2 Gas separation membrane

Our focus in this thesis is on gas separation membranes because separation through membrane has gained substantial consideration from different business areas as well as from research centers as it provides the most reliable and effective means of reforming environmental issues. Benny D. Freeman said, “Membranes will have a large role to play in important environmental and energy-related processes such as the cost-effective purification of hydrogen and methane”.

Major gas separation processes include:

- Oxygen and nitrogen separation from air

- Removal of hydrogen by different N_2 and CH_4 source
- Increasing the concentration of methane by separating it from numerous other components of biogas
- Separation of carbon dioxide, hydrogen suphide by natural gas

For these processes, we are to use membranes which must fulfill certain criteria. This was detailed by Baldus and Tillmman, who stipulated the following rules in favor of gas separation membranes:

- When desired purity is of moderate quality.
- When the products obtained after separation is of great importance.
- When feed gas is free from impurities and has no side effect on membrane surface.
- Membrane should have optimum selectivity for the successful achievement of desire separation.
- When feed gas can be introduced at any desire pressure and residue stream is needed at high pressure[4].

Gas separation membrane fabricating material should have some specific physical and chemical properties that can separate one component from mixture successfully. Membrane material must also have enough mechanical and chemical stability to remain functional for longer period of time. Gas separation characteristic of membrane influenced by:

- Material (separation factors: permeability and selectivity)
- Membrane morphology includes: surface and subsurface appearance and permeance
- Modification of membrane into module for commercial scale utilization (e.g. flat sheet, spiral wound, hollow fiber etc.)
- Membrane module[5]

A membrane's permeability and selectivity are defining parameters for better performance of gas separation. Here, permeability is define as the rate at which components can permeate through a membrane. Factors on which permeability depends are:

- Thermodynamic factor (separating of components from mixture when pass through membrane phase)
- Kinetic factor (diffusion of components through dense surface of membrane)

Next basic parameter is selectivity, innate characteristics of membrane to permeate one component preferentially than other from a mixture. It's also a vital parameter to acquire better product purity at high recoveries. If more selective membranes are being fabricated than gas separation membrane will grow enormously[6].

Material selection for the fabrication of membrane is one of the most significant step in separation processes. On the basis of desired chemical characteristics of material, certain choice of material is made for membrane fabrication. The effectiveness of separation of component from a mixture depends upon its interaction with the membrane material. If membrane material has certain functional groups which develop affinity towards particular gas from mixture, then one gas separates readily as compared to other and hence, it resulted in better separation efficiency of membrane. Membranes are made of a number of materials, namely ceramics, metals, glass and polymers [7, 8].

1.3 Inorganic membrane materials

Inorganic materials are one class of substances used for high temperature applications. Another class of materials are the organic or polymeric materials, which cannot be used at elevated temperatures. Intensive research has been done in developing membrane that can survive at high temperature and perform separation of gases components with their optimum limit. For this purpose, membranes were fabricated from inorganic materials which can be divided into three types: Zeolites, sol-gel based micro porous membranes and palladium based dense membrane.

Inorganic membrane are synthesized from silica, zeolite and carbon based molecular sieve, which are of greater importance because they have substantial chemical and thermal resistivity. However, these membranes have also some drawbacks; high manufacturing cost, reproducibility is difficult to achieve, highly brittleness, membrane area is low to module volume ratio, reduced permeability if selectivity increased of dense membrane i.e. metal oxides at temperature less than $400C^0$[9].

1.4 Polymeric membrane

Of all these materials, we selected polymers as our desired medium for membrane fabrication, because of the economic advantage they serve as well as the ease with which a membrane can be fabricated using polymers. Generally, polymers depicted increased selectivities and less through-put while relating to porous material because of less availability of free volume. Polymers can better transfer one chemical species over another in a mixture of gases. Knudsen diffusion and solution diffusion models govern the permeation of gases through porous and dense gas separation membrane respectively. In polymeric membranes increase in permeability will lead to decrease in selectivity and vice versa. Robeson, also set an upper bound limits for permeability/selectivity in a graph by plotting values of permeability obtained of small gaseous molecule mainly CO_2, N_2, CH_4 and O_2 permeates through polymeric membranes fabricated by different polymers. Usually dense or non-porous polymeric membrane are employed for gas separation. Gases are separated on the basis of their respective diffusion and solubility coefficient within polymer. Therefore, permeability is the product of solubility "S" of gas in membrane multiplied by the diffusivity "D" of gas in polymer. So permeation through non-porous polymeric membrane is through "solution-diffusion model" [10, 11]. Glassy polymers show more acceptability for fabrication of dense polymeric membranes to that of rubbery polymers, because former provide high selectivity and low permeability for different gas mixtures such as CO_2/CH_4, O_2/N_2 and H_2/CH_4.

Number of polymers have been tested for fabrication of dense gas separation membranes, but only a few have gained acceptance on industrial scale. In rubbery polymers polydimethyl siloxane and in glassy polymers cellulose acetate, polyurethane, polyimides, polysulfone and polyphenylene oxide are most common. Selection of polymer for gas separation membrane should provide optimum selectivity and high permeability for particular component in a mixture of gases[12].

Initially pristine polymers were used for the fabrication of membrane on lab scale and with successive triumphs on lab scale led to the fabrication of membrane modules of the same polymers on commercial scale. Cellulose acetate was the most common polymer employed for commercial purpose, in industrial plant in 1980[13]. In addition hollow fiber

module made from cellulose acetate were installed in Kelly-Snyder oil field for updating gas processing facility in 2006[14]. These module were made form pristine polymer and for further increase in permeability and selectivity some more modifications are necessary in gas separation membranes.

Later on, as research progressed, it was seen that polymeric materials are limited in their separation performance for gases, as far as current membrane technology is concerned. So, new materials were required for improving gas separation performance. Therefore, polymer blend membranes were suggested for improving gas separation performance. The biggest advantage of blend membranes is that they combine the favorable properties of two different polymers into one membrane. For example, one tough polymer can be combined with a highly permeable one, to give the benefit of high permeability as well as mechanical toughness. A blend can also be the combination of highly porous polymer with a highly selective polymer. Polymers blend can be either miscible, if dissolve in common solvent and immiscible if solution system is required for their solubility. Miscible polymer blend have uniform composition and appear in single phase and show single value of melting temperature and glass transition temperature[15, 16]. In immiscible polymer blend membrane polymers were dissolved in two different solvent and make solvent system for better performance. In immiscible polymeric blend the properties will depend on the phase distribution as well as the composition, and the different phases will act as separate pure polymers. Therefore, the polymer blends can be used when we need to combine the advantages of two different polymers. Of these two types of blends, immiscible polymer blends have the advantage of giving us better control of membrane morphology. This means that we can change the composition of the blend to see what effect it has on the morphology of the final membrane [16-18].

The current polymeric membrane materials are incapable of coping with the commercial scale requirement for separation of chemical species. If increase in permeability is achieved, then sudden decline in selectivity is observed and vice versa. An entirely new class of membrane materials were introduced by incorporating inorganic particle into polymers as filler particles, to make polymer/inorganic particle hybrid called mixed matrix membrane[19]. Inorganic particle have peculiar characteristics: specific pore size, pore

size of precise shape and geometry, tunable pore diameter and very close distribution of pore size. These inorganic particles act as molecular sieve to enhance diffusivity and selectivity, therefore polymer/inorganic particle hybrid gives better separation performance surpassing pure polymer and polymer blend membranes. Most common inorganic particle used are carbon nano-tubes CNTs, Zeolites and metal organic frame work MOFs[20, 21].

In one particular research work, mixed matrix membranes were fabricated by incorporating zeolites 4A into polymeric matrix including Matrimid and polyvinyl acetate for O_2/N_2 separation. Pore size range of zeolite 4A (3.8-4.0A) and reported selectivity for O_2/N_2 separation of 37 was reported and permeability of O_2 just 0.8 barrers. With this permeability and selectivity zeolite/polymer hybrid membrane gained significant attention but not considered for commercial purpose. This is because of poor interfacial compatibility, it results in the development of non-selective interfacial defect and low mechanical strength. On contrary, if concentration of zeolite is increased, then dispersion in polymer is non-uniform [22-24].

Therefore, currently research has been shifted from zeolite to other inorganic or organic particle such as grapheme base material, carbon nano-tubes and metal organic frame work.

1.5 Metal organic frame works

Metal organic frame work, MOF, is two or three dimensional compounds having cavities in it. According to IUPAC, *a metal organic frame work, abbreviated to MOF is a coordination network with organic ligands containing potential voids.* Coordination networks refer to a coordination compound ranging through repeating coordination entities in two or three dimensions. Another name for MOF is porous coordination polymer, which is defined by IUPAC as, *a coordination compound with repeating coordination entities in one, two or three dimensions[25].*

1.5.1 History of MOF

The history of MOF traced back to 1700 when a pigment called Prussian blue was synthesized. Its XRD analysis represented the three-dimensional network of Fe (II) and Fe (III) ions connected to CN^{-1} forming a cubic network structure. This highly organized

and symmetrical cubic topology encouraged chemists to synthesize more such compound with similar structure.

In 1990, a chemist named Robson anticipated the formation of a large compound composed of tetrahedral or octahedral metal nodes coordinated with linear shape organic ligand lead to the formation of material with the following characteristics:

- Compound having highly crystalline, potential cavities, possess chemical, thermal and mechanical stability with low mass to volume ratio.
- The presence of cavities within molecule capable of stores, permeate and separate guest molecules
- These frameworks were capable of post-modification in its organic part i.e. chemical up gradation of ligand by replacing or incorporation by different nucleophile or electrophile.
- In heterogeneous catalytic application, these compounds possessed catalytically active sites for specific reaction to take place.
- Cooperative catalytic activity possess between different catalytic sites.

So far, enough research has been done in the field of metal organic framework that most of the assumptions that were in theory in the 1990s are now transformed into real time applications.

MOF is the term used as distinguished class of compound first introduced by Yaghi in 1995, but two compounds $Cu_2(4,4'\text{-bipy})_3(NO_3)_2$ and Co(btc)(pyridine) synthesized at that time did not fit properly in the mof category. The first coordination compound which gained the status of MOF was synthesized in 1999 by Yaghi and Williams were: MOF-5 and HKUST-1 [26-30].

1.5.2 Characteristics of MOF

MOFs can be synthesized with revolutionary high porosity and internal surface area equal to 10000 m^2/g, and capable of tunable pore structure. In addition, they are chemically and mechanically stable towards acidic gases. Comparing MOF with zeolites, organic ligand in MOF have tunable pore structure, permitting superior interaction with polymers, thus diminishing nonselective deficiencies in MOF-polymer interface. Hence new

methodologies being adopted to form MOF-polymer mixed matrix membrane that have better gas permeability and selectivity [31]. So far, a number of MOF have been synthesized and explored for their diverse applications for instance molecular recognition [32, 33], separation properties [34, 35], gas storage [36] and delivery of required component of drug in pharmaceuticals industry[37]. Following are the most commonly used MOF in different applications owing to their peculiar characteristics and also used as filler in fabrication of MOF-polymer membranes i.e. HKUST-1, ZIF-8, MIL-53, MOF-74 and Gamma-CD-MOF.

HKUST-1 acronym for Hong Kong University of Science & Technology, HKUST-1, Chemically, this is synthesized by linking Cu^{2+} coordinated with benzene-1,3,5-tricarboxylate (btc) ligands. It has cubic structure with twisted boracite topology having main pore channel diameter of 9A (Angstrom) enclosed by tetrahedral pockets of 5A diameter. It has significant thermal stability up to $300C^0$ in nitrogen environment, moreover its metal site are open or coordinative unsaturated and rapidly exposed by temporary linked solvent or water molecule due to solvent exchange or some thermal procedure. Coincidently, these coordinatively unsaturated metal sites have an additional capability for gas sorption and act as Lewis acid in comparison to their coordinated saturated equivalent. HKUST-1 having particle size~ 10µm was used as filler in Matrimid and Matrimid/polysulfone blend to make asymmetric MMM by Basu et al, for carbon dioxide separation. Because of large particle size of HKUST-1, it had been difficult to fabricate defect free membrane and these defects between polymer and HKUST-1 resulted in unsatisfactory separation of mixture of gases. With another polymer, HKUST-1/6FDA-Durene MMMs and also the incorporation of ionic liquid result in considerably better permeability and selectivity values of CO_2/N_2 of 1100 barrers and selectivity of 27, and in case of CO_2/CH_4 selectivity of 29, as compared to pristine 6FDA-Durene membrane[27, 38-42].

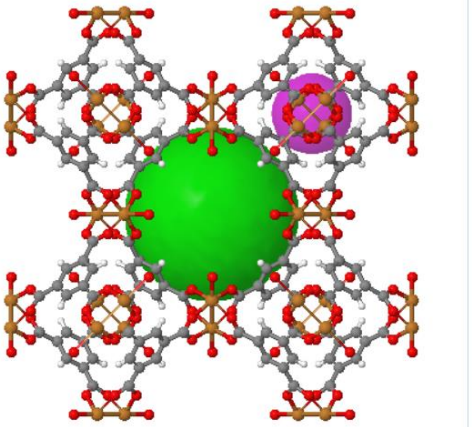

[43]

Figure 1: HKUST-1 MOF

ZIF-8 acronym for Zeolitic imidazolate frame work. ZIFs are synthesized by linking zinc or cobalt tetrahedrally coordinated to imidazolate linker. Because of similarity in bond angle and topology with zeolites, they are called Zeolitic. ZIF-8 is most abundantly used among subclass of ZIFs in gas separation membranes, because of its crystallographic characteristics having pore aperture of 3.4A and cages of 11.6A. The pore aperture of 3.4A act as molecular sieve for separation of gas from a mixture and allow them to permit through it especially that have kinematic diameter greater than 3.4A i.e. C_3H_8, C_3H_6 to diffuse from ZIF-8 pore aperture. For the separation of C_3H_6/C_3H_8 ZIF-8 incorporated into 6FDA-DAM polyimide and fabricate mixed matrix membrane. The particle size of ZIF-8 is around 600 nm in diameter and it disperse homogenously in polymer matrix and being hydrophobic in nature it require hydrophobic polymer for its dispersion and 6FDA-bases polyimide are of hydrophobic in nature and it resulted in permeability of 57 barrer in case of C_3H_6 and selectivity of C_3H_6/C_3H_8 31. 260% improved in permeability and 150% improved in selectivity of zif-8/6FDA-DAM as compared to pure 6FDA-DAM [44-47].

[48]

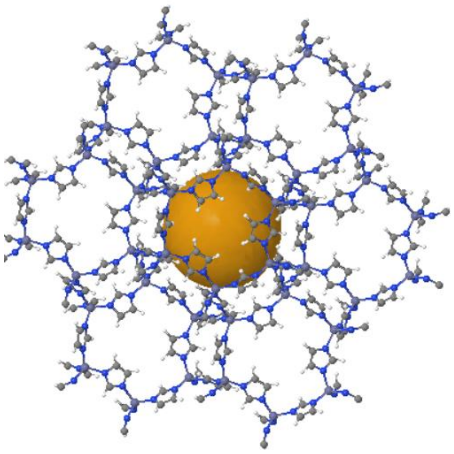

Figure 2: ZIF-8

MIL-53 stands for Material Institute Lavoisier mof fabricated by linking Aluminum, chromium, iron and scandium with terephthalic acid i.e. 1, 4-benzenedicarboxylate ligand [49-51]. It has three dimensional structure and pore size up to 8.5A. It has unique property of being elastic and have capability to contract or expand its pore size during the adsorption and desorption of certain gases i.e. CO_2. MIL-53 fabricate by Cr^{3+} metal ion with terephthalic acid have pore aperture of 29 & 34A have chemical, thermal and humid environment stability. For the separation of CO_2/CH_4 a MMM synthesized by incorporating ZIF-8 filler in 6FDA-DAM and result in permeability of carbon dioxide 660 barrer in CO_2/CH_4 with selectivity of 28[52-54].

[53]

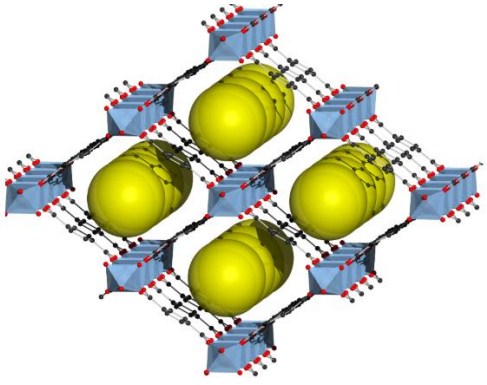

Figure 3: MIL-53

MOF-74 generally mentioned as M_2 (dobdc), and it's comprises of magnesium Mg, iron Fe, nickel Ni, copper Cu and zinc Zn as metal cation coordinated with 2, 5-doxide-1, 4-benzenedicarboxylate (dobdc) ligand having 12A wide hexagonal channels[55, 56]. Having maximum unsaturated coordinatively active metal sites act as Lewis acid and dramatically intensified gas adsorption[57]. MOF-74 extensively used in fabrication of MMM for CO_2 removal by integrating in polyimide base polymers. Very distinct features observed of MOF-74 in MMM as it enhanced plasticization resistance and selectivity for mixed-gas separation. MOF-74 with nickel as metal cation Ni_2 (dobdc) have large number of unsaturated active metal sites which help in increase in glass transition temperature in Ni_2 (dobdc)/6FDA-DAM MMM for C_2H_4/C_2H_6 separation up to T_g = 397C while T_g = 393C in case of pure 6FDA-DAM[58].

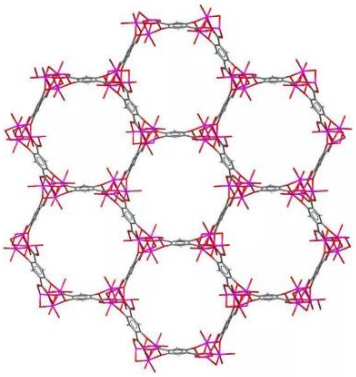

[59] Figure 4: MOF-74

In recent times an environment friendly and renewable MOF has been reported, this MOF also called green MOF as it is prepared from natural raw material, i.e. starch. Basic raw materials for this MOF are γ-cyclodextrin (γ-CD) and alkali metals salts mainly potassium hydroxide (KOH) and this MOF is called "Gamma-CD-MOF". The method involved for the preparation of this MOF is "vapor diffusion method" [60, 61]. This gamma-CD-MOF has a porous framework having body-centered cubic structure, with aperture of 7.8 A and cavity size of 17 A. In this MOF, potassium cation coordinatively bonded with –OCCO- unit present in D-glucopyranosyl ligand of gamma-cyclodextrin unit[62]. Gamma-CD-MOF has the ability to use for particular gas storage and adsorption from mixture of gases.

Because of ideal cavity size of 1.7nm and presence of three hydroxyl groups on each glycosidic ring and total of 24 hydroxyl group in single crystal of gamma-CD-MOF. Major application of gamma-CD-MOF are separation of halo aromatic compound, separation of saturated, unsaturated and chiral aromatic and alicyclic compounds, separation of benzene and toluene and also removal of CO_2 from natural gas also subject of extensive research on lab scale and efforts are being made to implement at industrial level[63].

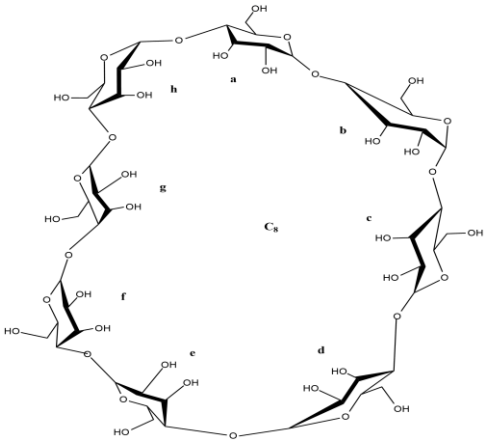

[64]

Figure 5: Gamma-CD-MOF

1.6 Selection of polymer

Now to practically implement the application of MOF for gas storage, gas adsorption and separation of organic compound from mixture, by incorporating powder form of MOF into certain continuous or large phase of polymeric matrix, where its effectiveness can be increased many-fold. MOF being crystalline, loses its crystallinity and flexibility, if employed in powder form for gas adsorption. So its efficacy can be retained by integrating into polymeric matrix and fabricating MOF-polymer MMM.

For fabrication of polymer/MOF MMM, we have selected two polymers, i.e. cellulose acetate and polyurethane and incorporate gamma-cyclodextrin metal organic frame work as filler. After fabrication these membranes undergo permeation testing for single gas and mix gas of CO_2 and CH_4.

1.6.1 Cellulose acetate

Most common polymer for membrane synthesis is cellulose acetate, its chemical structure is shown in figure (). Cellulose acetate is said to be primitive polymer for fabricating membrane for the removal of CO_2 from natural gas. Moreover on commercial scale membrane module are installed for the gas separation and these membrane module are CA based membranes i.e. "UOP's spiral bound membrane module" (600000 Nm^3/h) for carbon dioxide separation and similarly "Cynara-NATCO's hollow fiber membrane module" for offshore gas separation applications. For achieving better CO_2/CH_4 separation CA-based membrane have hydroxyl (-OH) and carbonyl (C=O) group in CA main chain and these groups induce more affinity towards CO_2. As described in earlier paragraph about γ-CD-MOF, a green metal organic framework adsorb CO_2. This MOF is now incorporated in cellulose acetate matrix as filler and CA/γ-CD-MOF mixed matrix membrane is fabricated. This membrane then undergoes permeation study of CA/γ-CD-MOF hybrid membrane for carbon dioxide and methane[65, 66].

1.6.2 Polyurethane

Another polymer used under detailed study in this research is polyurethane, a co-polymer composed of organic unit linked by urethane linkage. Polyurethane membranes have low selectivity but high gas permeability. Intensive research is underway, in order to increase the selectivity for a particular gas species, by either modifying PU internal structure or incorporating some nano-particles that optimize both selectivity and permeability. Many different nano-particles were incorporated and the permeability and selectivity of CO_2, CH_4 and N_2 were tested. In this research study γ-CD-MOF was introduced into PU matrix and PU/γ-CD-MOF MMM was fabricated and analyzed for its permeation, mechanical properties and pore structure[67].

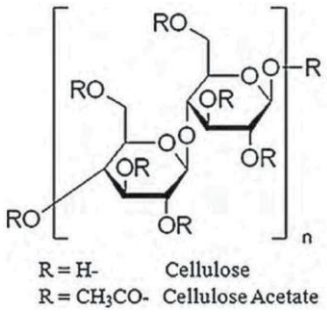

Figure 6: Cellulose Acetate structure

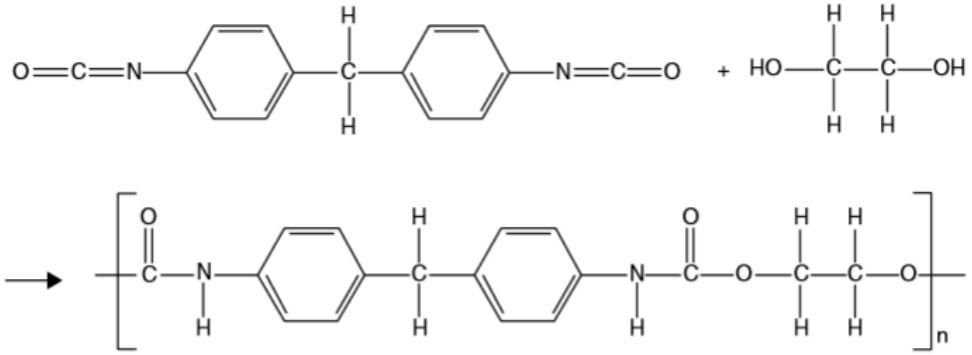

Figure 7: Polyurethane structure

1.7 Motivation

Metal organic frame work has been used extensively for carbon dioxide adsorption in different conditions. Gamma-CD-MOF also been tested for adsorption study and give satisfactory results. Therefore it is been advised to use γ-CD-MOF as filler and incorporated in polymeric matrix and fabricate polymer/γ-CD-MOF mixed matrix membrane. Furthermore, this mixed matrix membrane undergo permeation study for single and mixed gas testing for CO_2 and CH_4. The aim of this work is to incorporate γ-CD-MOF into polymeric matrix and fabricate mixed matrix membrane and enhanced the permeability and selectivity of CO_2 and CH_4. This will help in better separation of CO_2 from CO_2/CH_4 mixture.

The core objective of this research is:

- Optimize the weight percentage of filler concentration in polymeric matrix
- Fabricate pure polyurethane and PU/γ-CD-MOF mixed matrix membrane
- Fabricate pure cellulose acetate and CA/γ-CD-MOF mixed matrix membrane
- Permeability and selectivity measure of CO_2 and CH_4 from CA/γ-CD-MOF and PU/γ-CD-MOF matrix membrane
- Characterization of the resulting membrane by using the following technique
    - Scanning electron microscopy analysis (SEM)
    - Fourier transform infra-red microscopy FTIR
    - X-ray diffraction XRD

    - Mechanical testing from UTM
- Finally after getting results from both polymeric mixed matrix membrane, we compare these results with already publishing literature and also predict future recommendation for optimizing permeability and selectivity of CO_2 and CH_4.

1.8 Outline of the Thesis

1st Chapter details the introduction of metal organic frame works, their properties and their use in the adsorption of different gas. This chapter also include the incorporation of metal-organic frameworks (MOFs) into different polymers and their uses in making mixed matrix membranes for gas separation. Then, brief introduction of gas separation membranes, polymers employed for gas separation membranes. Finally, γ-CD-MOF also studied to see their use in mixed matrix membranes and cellulose acetate and polyurethane also studied in detail.

2nd Chapter includes examples of the research work carried out in the use of γ-CD-MOFs, polyurethane and cellulose acetate mixed matrix membranes for gas separation.

3rd Chapter summarizes the experimental techniques used to synthesize the mixed matrix, and also the characterization techniques used to study their various physical and chemical properties.

4th Chapter studies the results obtained from different characterization techniques for all the synthesized membranes, and these results are then discussed in detail to explain their significance in my work.

5th Chapter gives a concise summary of the entire work and also lists recommendations for future work

Chapter 2

Literature review

The increase in concentration of carbon dioxide in atmosphere will rise to increase in greenhouse gases that become the cause of global warming. Efforts are being made all over the world to reduce CO_2 concentration in atmosphere by different procedures i.e. by carbon dioxide sequestration, separation of carbon dioxide from natural gas through membrane system etc. most efficient process is through membrane separation. And membrane are being employed for its separation, among membrane system mixed matrix membrane gain significant appreciation and most widespread topics among researcher.

2.1 Metal organic frame work

Metal organic frame work has achieved tremendous acceptability in the last 15-20 years. Basic components of mof are: metal ions and organic ligands or linker. These metal ions and organic linkers have too much diversity and that results in assembling into different morphologies and crystalline structure[68]. In addition mof have remarkably high porosities, tunable but uniform pore size and high absorption capacity. That's why mof is under extensive research in chemistry, chemical and material engineering fields [69-71]. Major areas where there is potential to use mofs are: gas storage, separation of mixture of gases, as catalyst, sensing and proton conduction and others.

One of the most common application of mof is to use for the separation of mixture of gases. As separation of mixtures is the most vital unit process or unit operation in the chemical industry and require energy intensive process for its accomplishment. And separation of gas mixtures have more significance in chemical industries, most common gas separations includes: CO_2 capture (CO_2/air, CO_2/H_2), removal of acidic gases from natural gas (CO_2/CH_4, N_2/CH_4, and CO_2/H_2S), O_2/N_2 separation, separation of light hydrocarbons (olefin/paraffin), and noble gas separation and so on so forth.

2.2 Recent development in membrane technology using MOF

The detailed study of some common MOFs in their physical and chemical aspect as well as in their adsorption capacities are following: Zn_4O (BDC) $_3$ (MOF-5)[68, 72], Zr_6O_4 (OH) $_4$ (BDC) $_6$ (UiO-66)[73, 74], Al (OH) (BDC) (MIL-53)[52], Cu_2 (BPTC) (NOTT-100)[75], Cu_3 (BTC)$_2$ (HKUST-1), MIL-101(Cr) and so much more.

For adsorption of particular component in mof, it should have some adsorption capacity. It's divided into two basic categories i.e. gravimetric uptake and volumetric uptake. Amount of gas adsorbed within a unit mass of material called gravimetric uptake, whereas volumetric update defined as "volume of gas adsorbed under standard condition divide by volume of adsorbent". Mass of particular MOF required for gravimetric uptake and volume of adsorbent required comes under volumetric uptake. For the separation of one component from a mixture over the other component the MOF should be highly selective for one component than other. So adsorption selectivity defined as by following equation:

$$S_{12} = \frac{X_1 Y_2}{X_2 Y_1}$$

Y_1: mole fraction of component *i* in the bulk gas

X_1: mole fraction of component *i* in the adsorbed gas[76]

With the separation characteristics of MOFs as well as the mechanism explained above, the different MOFs with their selectivity and adsorption capacity are summarized in the table below:

Table 1: adsorption capacity and selectivity of CO_2/CH_4 for few MOFs

MOF	Surface area (m^2 g^{-1})	CO_2 uptake (mmol g^{-1}) at 1.0 bar	Selectivity CO_2/CH_4	Temperature (K)	Reference
Qc-5-Cu-sql-β	221	48	3290	292	[77]

SIFSIX-3-Zn	252	2.56	230	298	[71]
NENU-520	386	2.71	12.8	298	[78]
UTSA-16	627	2.36	29.7	298	[79]
MgMOF-74	1494	6.1	104	298	[79]
SIFSIX-2-Cu-i	734	6.1	34	298	[71]
UPC-12	270	1.5	691	298	[80]
PEI-MIL-101-125	183	4.35	230	298	[81]

Table 2: high pressure CO_2 adsorption capacity in MOF at temperature range 273-313K

Chemical formula	Common name	Surface area BET (m^2/g)	Capacity (wt %)	Pressure (bar)	Temperature (K)	Ref
$Zn_4O(BBC)_2(H_2O)_3$	MOF-200	4528	74	48-50	300	[82]
Cu_3(TCEPEB)	NU-100	6142	70	38-40	297	[83]
$Zn_4O(BTB)_2$	MOF-177	4490	61	48-50	297	[82]
$Cu_3(BTC)_2$	HKUST-1	1268	43	300	313	[84]

Table 3: at low pressure CO_2 adsorption capacities of MOFs at 292-320K

Chemical formula	Common name	Surface area BET (m^2/g)	Capacity (wt %)	Pressure (bar)	Temp(K)	ref
Co_2(dobdc)	Co-MOF-74	956	25	1	298	[85]
Zn_2(dobdc)	Zn-MOF-74		20	1	295	[85, 86]
$Zn_4O(BTB)_2$	MOF-177		6.7	1	299	[86]
$Cr_3O(H_2O)_2F(BDC)_3$	MIL-101(Cr)	2673	4.1	1	318	[87]

2.3 Gamma-Cyclodextrin-MOFs

Precursor for cyclodextrin molecules are carbohydrates mainly cyclic oligosaccharides, further divided into three types on the basis of the number of glycopyranose units, i.e. if six units called α-cyclodextrin, seven units called β-cyclodextrin and eight units called γ-cyclodextrin. These glycopyranose units are linked by α-(1-4) bonds. These cyclodextrin were discovered in 1891, accidently in starch digest of *Bacilus amylobacter* as crystalline material along with reducing dextrin. Before 1942 structure of α, β-cyclodextrin were unknown and after the invention of X-ray crystallography their structure finally revealed. In 1948 γ-cyclodextrin structure was also found out by X-ray crystallography and it was predicted that cyclodextrin can form inclusion complexes. Because of making inclusion complexes with different compounds, cyclodextrin gained sufficient preference. X-ray structure provided detailed symmetry of cyclodextrin ring, secondary –OH group (C_2 and C_3) located on broader edge of ring and primary –OH group (C_6) on other edge of ring. Polar or non-polar C_3 and C_5 hydrogen and ether like oxygen located at inside of torus-like molecule. This resulted in hydrophilic cavity outside that can dissolve in water and hydrophobic from inside forming a “micro-heterogeneous environment” [88-93].

Table 4: Comparison of α, β, γ-cyclodextrin properties[93]

Properties	α-cyclodextrin	β-cyclodextrin	Γ-cyclodextrin
No. of glycopyranose ring	6	7	8
Molecular weight (g/mol)	972	1135	1297
Solubility in water at 25C (w/v)	14.4	1.84	24
Outer diameter (A)	14.5	15.3	17.4
Cavity diameter (A)	4.6-5.2	6-6.4	7.4-8.2

Gamma-Cyclodextrin-MOF gained more acceptability due to ease in its synthesis from γ-CD and potassium hydroxide (KOH) by vapor diffusion method. Γ-CD-MOF acquired body centered cubic structure with aperture 7.8 angstrom, have spherical voids having diameter of 17 angstrom. Potassium cation (K^+) linked with –OCCO- units of D-glucopyranosyl residue of γ-cyclodextrin. The γ-CD-MOF used for the adsorption of different gases e.g. CO_2, CH_4, N_2 and H_2[94]. In addition also employed for the separation of organic compound especially of benzene family i.e. BTEX (benzene, toluene, ethyl benzene and xylene) with greater selectivity. Furthermore, separation of paraffin and olefin, aromatic and alicyclic and halo aromatic compound also achieved through γ-CD-MOF[95].

CD-MOF-2 have chemisorptive process of binding CO_2 at low pressure showed greater affinity for carbon dioxide. In case of CO_2/CH_4 the conditions for better selectivity of adsorption of CO_2 over CH_4 is on low pressure <1 Torr and at temperature range 273-298K and followed chemisorption mechanism with selectivity of adsorption of CO_2 over CH_4 achieved around 3000fold[96, 97]. Jeremiah J. Gassensmith et.al explained the adsorption of CO_2 is preferable at low pressure. The adsorption of CO_2 on CD-MOF-2 is categorized under chemisorption because of affinity of hydroxyl group present in CD-MOF-2 structure with carbon dioxide. This –OH group support as reactive spot for the synthesis of H_2CO_3 due to chemisorption phenomena which takes place with CO_2. The better selectivity of CO_2 over CH_4 is due to exceptional nano-porous crystalline structure of CD-MOF-2. This promising feature of CD-MOF-2 is due to its synthesis from starch (carbohydrates), a green and environmentally friendly material having neutral carbon

atom and good carbon dioxide absorbing capacity and considering suitable material for carbon fixation [63]. Moreover, the porosity and storage properties of CD-MOF-2 were experimented by performing gas sorption analysis of following gases i.e. N_2, H_2 and CH_4. The different isotherms were made for the analysis of sorption of gas by CD-MOF-2. First nitrogen isotherm demonstrated sharp uptake at low pressure region in low pressure region of 1 bar at 77K with capacity of 252 cm^3g^{-1}, agreeing with BET surface area of 1030 $m^2 g^{-1}$ and pore volume of 0.46 g cm^{-1}. More ever isotherm for H_2 showed intermediate storage capacity around 90-100 cm^3g^{-1} with pressure and temperature of 1 bar and 76K respectively[63, 98].

2.4 Polyurethane mixed matrix membrane

Behnam et.al studied the permeation of CO_2, CH_4, O_2 and N_2 through pure polyurethane membrane and polyurethane-mesoporous silica membrane. MCM-41, MCM-48 and SBA-16 silica blend with PU to fabricate PU-silica mixed matrix membrane. The increase in filler weight percentage resulted in increase in permeability but reduction in selectivity observed. Due to presence of mesoporous silica in polyurethane gas molecule follow Knudsen diffusion regime. This caused higher permeability in PU/mesoporous-silica then in pure PU. Best sample is MCM-48 mesoporous silica-PU hybrid, with permeability of CO_2 and CH_4 at 45.3 and 8.1 barrers respectively and selectivity of 5.6 for CO_2/CH_4 [99]. Moreover, Banafsheh Soltani and Morteza Asghari studied the gas separation of polyurethane by incorporating zinc oxide ZnO nano-particles and synthesized MMM. Zinc oxide as filler enhanced the mechanical, physical and optical properties of polymeric mixed matrix membrane. Different weight percentage of PU/ZnO sample were prepared and permeability calculated of CO_2 and CH_4 at 4 bar of 37.73 & 3.52 barrers, at 8 bar of 57.79 & 3.76 barrers, and at 12 bar, values of 69.09 & 3.77 barrers respectively, in case of neat polyurethane membrane. Most optimum results were obtained from PU-ZnO 0.50 wt. % with increase in permeability of CO_2 for loading approximately up to 30% and selectivity of CO_2/CH_4 at a value of 19.76 (permeability at 4 bar of 55.23 barrers, at 8 bar of 69.31 and at 12 bar of 80.72 barrers) to that of pure polyurethane. The increase in permeability of CO_2 is due to the following factors: polar nature of carbon dioxide molecule, small kinetic diameter (3.30A), better condensability and higher affinity of CO_2

molecule with polar group in PU matrix. With further addition of ZnO (up to 0.75 wt% and 1.0 wt% of PU) resulted in decline of permeability of CO_2[100].

Furthermore, gas separation properties of polyurethane were investigated by addition of silica, ZSM-5 and ZIF-8 nano-particles. All these have different particle and pore size and have varying effect on the permeability and selectivity of CO_2 and CH_4. More focus was given on ZIF-8, because of its high chemical and thermal resistivity, pore size in between to kinematic diameter of methane and carbon dioxide i.e. 0.34 nm, so it assumed to act as molecular sieve and showed more affinity towards CO_2. By increasing the weight percent of silica into polyurethane improvement in selectivity from 15 to 23 is also observed for CO_2/CH_4. This is because the silica particles fill the free spaces in the polymeric chains of polyurethane and lessening in permeability of larger particle is witnessed i.e. of methane. But less lessening in permeability of CO_2 appeared and hence selectivity increased. The incorporation of ZSM-5 in PU resulted in two different behavior in the permeation of gases, with increasing concentration up to 5% resulted in better permeability and selectivity of gases. Because ZSM-5 caused some variation in PU structure by introducing some void spaces that lead to dissolution of gases with more solubility and increased sorption selectivity. As ZSM-5 pore size is approximately 5A, larger than kinetic diameter of both CH_4 and CO_2 so further addition from 5% to 20% lead to enhancement of CO_2 permeability from 46 to 117 while selectivity decreased. Best results were achieved from PU/ZIF-8 10 wt% with permeability 74 barrers and selectivity of 20 of CO_2/CH_4[101].

Elham Ameri et.al studied the permeability and selectivity of O_2, N_2, CO_2 and CH_4. It was found that good results were obtained with polyurethane synthesized with BDO and MPD chain extender with 30 wt% alumina nano-particles. Permeability gained in B-30 was CO_2 78 and CH_4 3.95 barrers and selectivity of CO_2/CH_4 is up to 19. Similarly, in case of M-30 permeability of CO_2 is 74 and of CH_4 is 3.18 barrers and selectivity of CO_2/CH_4 of 23. By enhancing the weight percentage of alumina nano-particles in PU causes decrease in permeability of all gases. Increase in alumina content acts as impediment in passing of gas molecules by increasing gas diffusion path length[102]. Further enhancement of gas separation was being investigated by assimilation of epoxy nano-particles in polyurethane.

So far inorganic nano-particle incorporated into PU and organic epoxy nano-particle now integrate into polyurethane matrix and gained better permeation value for carbon dioxide. Similarly with higher concentration of epoxy nano-particle (PU/EP-20 and PU/EP-30) reduction in permeability is achieved. With enhancement of epoxy content in PU, number of hydroxyl groups increases which have more affinity with CO_2. So carbon dioxide now becomes more soluble in PU/EP composite membrane as to that of methane. The high selectivity of CO_2/CH_4 because of following reasons:

- Due to presence of filler in polyurethane matrix it creates narrower pathways that hindered the permeation of large molecule and permeability of CO_2 increase and hence selectivity too.
- Presence of hydroxyl group (-OH) in PU and of epoxy nano-particle showed more affinity towards carbon dioxide and lead to more solubility of CO_2 and increase in selectivity appeared[103].

Table 5: summary of filler in PU matrix

Serial no.	Polymer	Filler	Permeability and selectivity	Reference
1	PU	Mesoporous silica PU/Silica MCM-48	CO_2 = 45,CH_4 = 8.1 CO_2/CH_4 = 5.6	[99]
2	PU	Zinc oxide nano-particle ZnO PU/ZnO 0.50 wt.%	CO_2 = 55,CH_4 = 3.8 CO_2/CH_4 = 14.5	[100]
3	PU	SiO_2 Zeolite ZSM-5 ZIF-8	CO_2/CH_4 = 23, CO_2/CH_4 = 3.3 CO_2/CH_4 = 20.6	[101]
4	PU	Alumina nano-particle	CO_2 = 78 CH_4 = 3.95 CO_2/CH_4 = 19.3	[102]

5	PU	Epoxy nano-particle	CO_2 = 134 CH_4 = 8.2 CO_2/CH_4 = 16.4	[103]

2.5 Cellulose acetate mixed matrix membrane

Hamidreza et.al calculated the permeability through cellulose acetate/non-porous zeolite mixed matrix membrane for the separation of CO_2/N_2. Reason for fabricating membrane with cellulose acetate was due to it being the most common and earliest polymer membrane material for CO_2 separation from N_2 and CH_4. Moreover, on commercial scale large spiral-wound membrane module was also fabricated using CA as base matrix. Hollow fiber membrane module installed on off-shore installations for separation of CO_2 from natural gas was also fabricated from cellulose acetate. CA also had peculiar characteristics of developing affinity with the filler incorporated for fabricating CA/filler mixed matrix membrane. In this paper, NaY zeolite was incorporated in to CA matrix and CA/NaY zeolite solution was cast on clean glass plate and thickness controlled by using doctor blade. By increasing NaY zeolite concentration from 0 to 20 wt%, increase in CO_2 permeability was observed, but after further enhancement of filler concentration (up to 25 wt %), decrease in permeability was observed for CO_2. Maximum increase in permeability observed for CO_2 is 4.9 barrers, and decrease in CO_2/N_2 selectivity from 26 to 18 with the loading of 0 to 15 wt%. Maximum selectivity achieved at 20 wt% filler loading and then sudden decline appeared due to percolation effect of particle in membrane matrix. The lesser rise in diffusivity selectivity concurrently with greater decline in solubility selectivity in CA/NaY zeolite MMM is due to agglomeration of higher concentration of filler. Then, there is influence of increase or decrease of pressure on the permeability of CO_2, as increase in pressure led to reduction in permeability of glassy polymer. This decrease in permeability can be explained by dual sorption model[104].

Multi walled carbon nano-tubes assimilating into cellulose acetate matrix and fabricating hybrid membrane and calculated the permeability and selectivity of CO_2 and CH_4. In this paper, carbon nano-tubes (CNTs) have been tested with acetone and incorporated into cellulose acetate matrix along with polyethylene glycol. PEG improves the chain

flexibility and MWCNT aids thermal stability, mechanical stability and long tortuous pathway for permeation of carbon dioxide. The permeation behavior of gases divided into two sections, first effect of PEG and PEG/MWCNT wt% on single and mixed gas permeability, as well as CO_2/CH_4 selectivity and second effect of pressure on the permeability and selectivity of CO_2/CH_4. Neat CA has more permeability for CO_2 and CH_4 as compared to CA/PEG blend membrane. Because cellulose acetate contained neutral voids between the polymeric chains endorsed by irregular arrangement of chain resulted in the creation of free volume that is responsible for increased permeability of both CO_2 and CH_4 and drop in selectivity of CO_2/CH_4. MWCNT added in CA from 5 to 15 wt. % keeping the weight percentage of PEG constant i.e. 10 wt. % and observed the permeability and selectivity of CO_2/CH_4. Increased selectivity was observed for CO_2/CH_4 from 2.15 to 28.66 for 10% PEG/CA and additional incorporation of 10% MWCNT escalated CO_2/CH_4 selectivity from 28.66 to 38.4. Similarly, with increase in pressure, permeability decreased, as very less flow occurs for gases due to higher pressure difference, as compared to high flow observed at lower pressure difference. Finally, 10%MWCNT / 10%PEG / CA gives best results for single and mixed gas selectivity of CO_2/CH_4 up to 48 and 38 respectively[105].

Cellulose acetate was also blended with Titania nano-particle (TiO_2) to study the permeation characteristics of both CO_2 and CH_4. One reason for selecting Titania is that it is distinctive type of semiconductor and it gives anti-fouling, thermal stability and mechanical properties to membrane when incorporated with polymer. Moreover, TiO_2 also when introduced in polymer matrix for studying gas permeation property of H_2/N_2, O_2/N_2, H_2/CO_2 and CO_2/N_2. In this paper CA/TiO_2 MMM was synthesized by diffusion induced phase separation techniques and penetration properties of CO_2 and CH_4 gases were experimented. With five different weight percentages, TiO_2 integrating in CA matrix and best selectivity achieved CO_2/CH_4 with 20% TiO_2[106].

A.R. Moghadassi et.al fabricated a blend of cellulose acetate with MWCNT MMM, CA/PEG/MWCNT and CA/styrene butadiene rubber (SBR)/MWCNT blend MMM by solution casting method. These membranes were used to study the permeability and selectivity of CO_2/CH_4. The MWCNT used as filler and these were further categorized in

two ways i.e. raw-MWCNT (R-MWCNT) and functionalized carboxylic acid-MWCNT (C-MWCNT). For increasing stress bearing property of membranes and also enhancing gas permeation performance, blend of CA with SBR used and incorporate MWCNT as filler. CA/MWCNT MMM prepared with different weight percentages of MWCNT and permeability of helium, nitrogen, methane and carbon dioxide and selectivity of CO_2/CH_4, CO_2/N_2 and N_2/CH_4 were tested at 2 bar pressure. Generally permeability increase with increasing MWCNT loadings of all gases and selectivity of $CO2/CH_4$ and CO_2/N_2 increase, but decrease in selectivity observed for N_2/CH_4. In case of CA/PEG/MWCNT increase in permeability witnessed at CA/PEG/MWCNT-1% sample for all gases and best selectivity obtained at CA/PEG/MWCNT-0.5% sample for $CO2/CH_4$, CO_2/N_2 and N_2/CH_4.in last sample of CA/SBR/MWCNTs optimum permeability achieved at CA/SBR/MWCNT-0.5% sample for all testing gases and best selectivity observed at CA/SBR/MWCNT-2% for $CO2/CH_4$ and CO_2/N_2 and CA/SBR/MWCNT-1% for N_2/CH_4[107].

Muhammad Mubashir et.al measured the permeability and selectivity of CO_2, N_2 and CH_4 from NH_2-MIL-53(Al)/CA MMM. As mentioned in literature, the incorporation of amine functionalized metal-organic frame work in polymeric matrix resulted in the enhancement of permeability of carbon dioxide as linked to pure MOF based MMM. NH_2-MIL-53(Al) an amine functionalized MOF having MIL-53 topology. Al^{+3} coordinated with amine group and acquire diamond shape having aperture of 7.4A. Some convincing properties to use as filler for gas permeation study are significant resistance against high temperature, optimize pore volume and considerable surface area. Furthermore, compatibility with polymer favors due to presence of terephthalate ligands in NH_2-MIL-53(Al). CA/NH_2-MIL-53(Al) mixed matrix membrane fabricated and permeation study conducted at 3 bar pressure and 25C temperature for CO_2, N_2 and CH_4 in case of pristine cellulose acetate permeability of CO_2, N_2 and CH_4 reported is 16, 1.7 and 1.4 barrers. After fabricating CA/NH_2-MIL-53(Al) MMM, significant increase in permeability measured as 52.6, 2.2 of CO_2 and N_2 respectively and selectivity calculated as 23.5, 2.3 of CO_2/CH_4 and CO_2/N_2 respectively[108].

Chapter 3

Experimental Methods

3.1 Materials used

Polyurethane in the form of pellets purchased from Sigma Aldrich, cellulose acetate CA with average molecular weight Mn = 50,000 GPC, from Sigma Aldrich, ultra-pure Tetrahydrofuran (THF) obtained from Sigma Aldrich (boiling point $65C^0$, density 0.89 g/ml). As prepared Gamma-cyclodextrin-MOF was obtained from another research student within the research group. Gas permeation testing of CO_2 and CH_4 acquired from Linde Chemicals with 99.99% purity of single gas respectively and also CO_2/CH_4 gas mixture used with 50:50 by volume.

3.2 Synthesis of pure polyurethane membrane

Pure polyurethane membrane was prepared by solution casting method, by dissolving PU in THF making 10% w/w polymer to solvent solution. The polymer-solvent solution was allowed to stirred overnight and making a homogenous solution. Afterwards the solution was cast on petri dish and allow solvent to evaporate at room temperature by keeping it in fume hood for next 24 hours. For further evaporation of solvent kept membrane in vacuum oven for 5-6 hours. The synthesized membrane with thickness of 100µm.

3.3 Synthesis of PU/γ-CD-MOF mixed matrix membrane

PU/γ-CD-MOF MMM were synthesized by incorporating different weight percentages of filler in polymeric matrix. Initially γ-CD-MOF was dissolved in different percentages from 0.2-1 wt. % of polymer in THF and left to stir overnight on magnetic stirrer. And pure PU 10% w/w (polymer to solvent) in separate vial in THF for 24 hours. After achieving homogeneity, both solution were mixed together and undergo sonication for 2 hours and then further stirred for 60 minutes before casting on petri dish. Similarly it would take 24 hour for complete evaporation of solvent and for complete removal of solvent membrane were transferred in vacuum oven for 5-6 hours at $60C^0$. The different membrane sample were prepared and tested for both single and mix gas permeation

testing. Further analysis of permeate from mix gas testing, gas chromatograph technique was used. Membranes undergo FTIR, SEM, XRD and UTM analysis.

3.4 Fabrication of pure cellulose acetate membrane

Pure cellulose acetate membrane was prepared by solution casting method. In this case 0.265 g CA dissolved in 4 ml Tetra Hydro-Furan (THF) solvent making 7.5 wt. % solution and allow to stir overnight. After the formation of homogenized solution cast on petri dish and allow solvent to evaporate at room temperature for next 24 hours. For complete removal of solvent kept petri dish in vacuum oven for 5-6 hours for 50-60C. Pristine CA membrane synthesized with membrane thickness approximately 40µm.

3.5 Synthesis of CA/γ-CD-MOF mixed matrix membrane

Mixed matrix membrane gives better permeability and selectivity for a particular gas from mixture of gases and also introduced mechanical stability to membrane. Gamma-CD-MOF in different weight percentages from 0.2-1 wt. % dissolved in separate vials in THF and CA in separate vial also in THF. After complete mixing of γ-CD-MOF in THF, add this solution in already dissolved CA+THF solution and co-sonicated it for 2 hour for complete and uniform dispersion of mof into CA matrix. Furthermore this hybrid polymer-filler solution stirred for 30-60 minutes and finally cast on petri dish. Allow 24 hour for removal of solvent and for complete removal of solvent kept petri dish in vacuum oven for 5-6 hours at 50-60C. CA/γ-CD-MOF mixed matrix membrane synthesized with membrane thickness approximately 50-60µm.

3.6 Testing and Characterization

3.6.1 Fourier Transform Infrared (FTIR) Spectroscopy

Fourier transform infrared is an analytical technique used for qualitative and quantitative analysis of the presence of functional group in organic compounds, detecting the type of chemical bond in molecule, explaining precise information about molecular structure and specifically for the recognition and determination of functional group in sample.

In FTIR when infra-red beam incident on sample, it is absorbed by the sample. A sample contain numerous energy states level. When molecule absorbed infra-red radiation these molecule jumps to higher energy states level from ground state. And wavelength it

absorbed proportional to transfer the molecule from ground to respective energy state. Different functional group present in a sample and absorb infra-red of different specific wavelength and it called fingerprint of that functional group. Now all the characteristic absorption peak of all functional group combine to complete the spectrum of sample and hence detail study can be done using FTIR spectrometer.

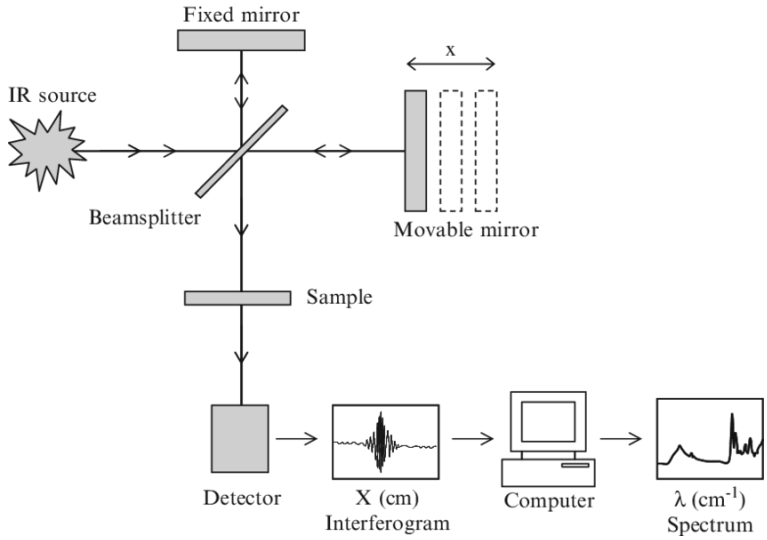

Figure 8: schematic diagram of FTIR Spectroscopy [109]

FTIR spectroscopy was performed on Perkin-Elmer Spectrum 100 FT-IR Spectrometer at wave number range of 4000-400 cm^{-1} and at resolution of 4 cm^{-1}. Gamma-cyclodextrin-MOF sample for FTIR was prepared by making suitable pallets with potassium bromide KBr and subjected to FTIR spectrometry. Membrane sample were tested by simply fitting membrane into sample cell and subjected to infra-red radiations. Presence of different functional group in membrane were studied using the spectrum[109, 110].

3.6.2 Scanning Electron Microscopy (SEM)

Scanning electron microscopy (SEM) is an analytical technique employed to study the surface topography and morphology of membranes, cross-sectional structure of membrane, pores geometry and crystalline structure of metal organic frame work.

Components of SEM:

- Electron generating source

- Column where electron moves along with electromagnetic lenses
- Electron detector
- Sample chamber
- Display screen or computer

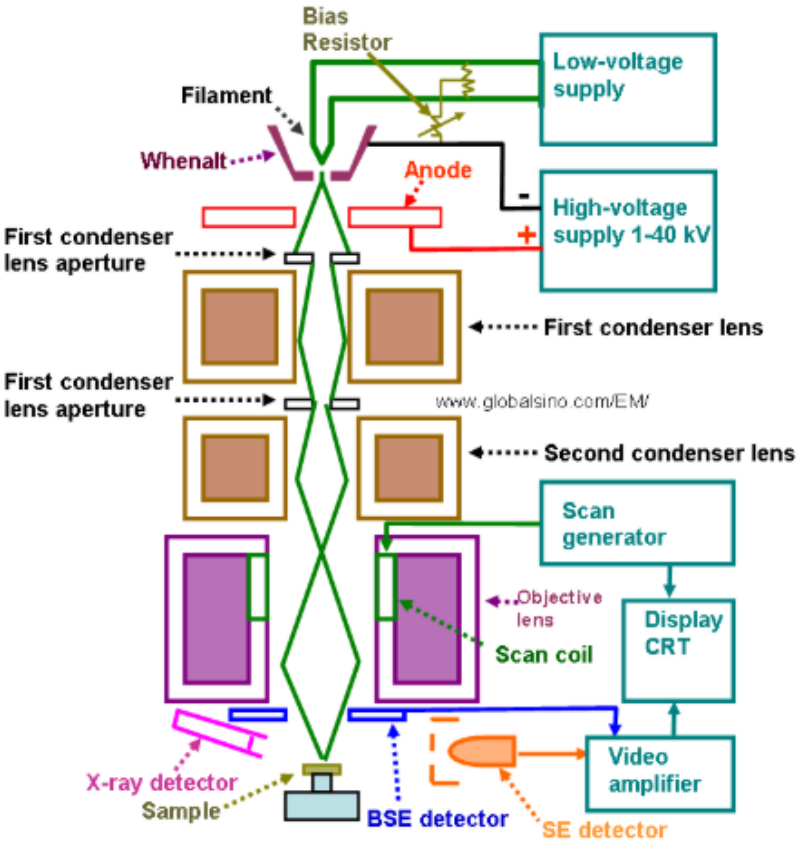

Figure 9: schematic diagram of SEM [112]

When electron beam is incident on sample, it aids in studying and examining the characteristics of specific area of sample with greater accuracy and precision. Signals generated between the interaction of electron beam and sample were received by the detectors and analyzed accordingly. SEM analysis is being performed on few sample by SEM (S-4700 Hitachi, Japan) and gold sputtering was performed on membrane by ion sputtering machine JFC-1500 of JEOL Ltd. And few sample were analyzed by "MIRA3 TESCAN system", with magnification of 5000x, 10000x, 20000x, 25000x and 30000x and voltage of 5Kv. All membrane sample including pure polyurethane and PU/γ-CD-MOF MMM and pure cellulose acetate and CA/γ-CD-MOF MMM samples of 0.2, 0.4,

0.6, 0.8 and 1 wt. % were undergo sem analysis and their best images of surface and cross-section were studied in detail[111, 112].

3.6.3 Ultimate tensile machine

Tensile strength of a material can be defined as the maximum stress that a material can stand before it attain a permanent deformation in its structure. Material are either glassy or rubbery on the basis of their mechanical strength. Ultimate tensile machine is used to calculate the stress bearing strength of pure and hybrid polymeric membranes.

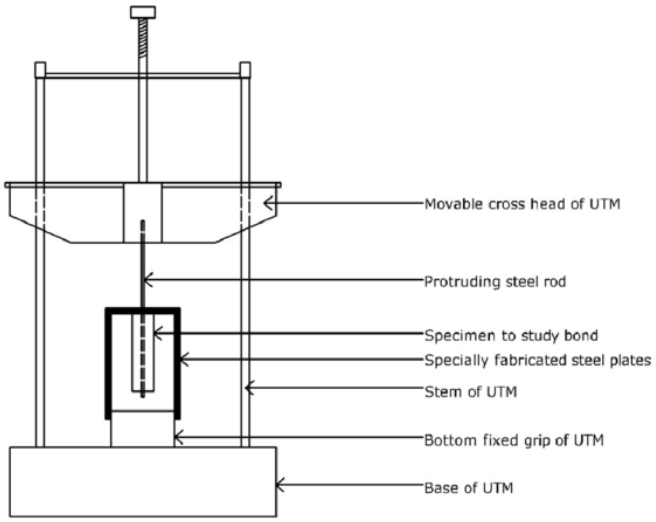

Figure 10: schematic diagram of ultimate tensile machine [113]

Tensile strength of pure polyurethane and PU/γ-CD-MOF mixed matrix membrane as well as pure cellulose acetate and CA/ γ-CD-MOF mixed matrix membrane samples of 0.2, 0.4, 0.6, 0.8 and 1 wt. % were tested using "SHIMADZU ADS-X" series precision ultimate tensile tester with a full load of 20KN. Samples were tested adopting ASTM standard D882-02 and strips were made according to the dimension mention in standard. Lastly detail study of sample were made after the results drawn from testing[113].

3.6.4 X-ray Diffraction

X-ray diffraction is an analytical technique that depends on dual wave/particle of x-ray to get the true picture of structure crystallinity. Most important task of this technique is the identification and characterization of compound present in sample. X-ray diffraction helps in find out size and shape of crystallites, phase purity, lattice parameters and crystallinity.

X-ray diffraction pure polyurethane and PU/γ-CD-MOF mixed matrix membrane sample and pure cellulose acetate and CA/γ-CD-MOF MMM samples of 0.2, 0.4, 0.6, 0.8 and 1 wt. % were done by equipment "STOE Germany". Scan angle was kept 5^0-60^0 with step size and step time was selected as 0.4 degree and 1 respectively. Radiation adopted for performing characterization was Cu K α-1. XRD were used to identify the d-spacing between structure layers at a specific angle as by Bragg's law

$$N\lambda = 2d \sin\theta$$

Bragg's law is simple to understand the process of diffraction and is generally used in crystal diffraction as well. By using Debye-Scherrer equation we can find the crystallite size of the crystals. All crystalline material has its individual unique X-ray pattern which is used as a finger print for its identification[114].

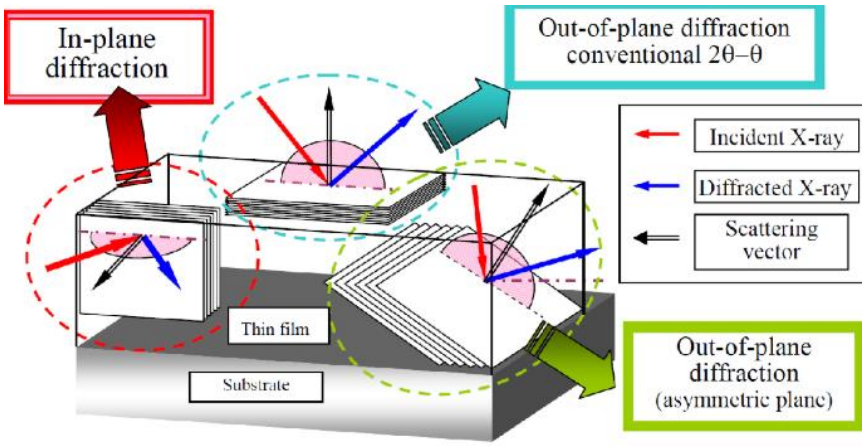

Figure 11: schematic diagram of XRD [114]

3.6.5 Working principle of gas permeation testing system

Gas permeation system is used to execute gas permeation experiment through the membranes. The permeability of gas passing through this system can be measured by the following relationship.

$$P = \frac{ql}{A\Delta P}$$

P: is permeability defined as: "measure of the ability of fluid passing through selective permeable medium". Permeability expressed in barrer (1 barrer = 10^{-10} cm^3 (STP) cm $cm^{-2}s^{-1}cmHg^{-1}$).

Q: flow rate of permeate gas passing through membrane cm^3/s

L: membrane thickness cm

ΔP: (p_1 and p_2) are the absolute pressure at feed and permeate side respectively

Furthermore ideal selectivity of gases can be found by the following formula: $\alpha_{A/B} = \frac{P_A}{P_B}$

For single gas permeation testing, a stainless steel gas permeation rig is used. The gas permeation rig is used for testing the permeance of gases through a membrane. The membrane is fitted into the membrane cell. Feed gas is introduced at the top of the cell while permeate is exited from the bottom of the cell. For the purpose of finding out the flow rate of permeate gas, a portion of that gas is taken through a bubble flow meter, in which the time taken for the bubble to flow a fixed volume gives us the gas flow rate.

For the purpose of single gas permeability testing, we have used the PHILOS Gas Permeability Test System which has stainless steel gas permeation rig in it. The membranes are tested for permeation of CO_2 and CH_4 gases at different gauge pressures, from 1 bar to 5 bars. After doing this testing, permeability of both gases and single gas selectivity are calculated.

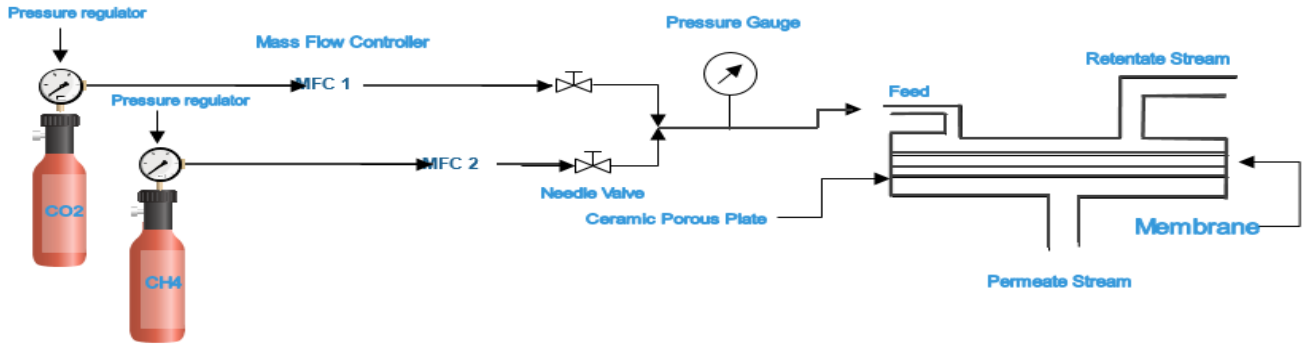

Figure 12: schematic diagram of gas permeation system

3.6.6 Working principle of gas chromatograph

Chromatography is a separation and analytical technique, in which a solution of two or more liquids or gases (the test sample) is fed in with a mobile phase, over a stationary phase. The stationary phase either solid or liquid adsorbed on a solid. The distribution of

the different components of the feed mixture between the stationary and mobile phases, helps in the separation and analysis of the components of the mixture. Chromatography can be classified on the basis of a number of classifications. One classification is on the basis of phases used, which includes liquid chromatography and gas chromatography. Gas Chromatography (GC) is a general, broad term used for any type of chromatography, in which gas is used as the mobile phase. It is categorized into gas-solid chromatography (GSC) and gas liquid chromatography (GLC).

For mixed gas permeation testing, gas chromatography (GC) is used. Permeate from gas permeation rig or permeation cell is connected to Gas Chromatograph, for analysis of composition of permeate coming out of the membrane. The composition of permeate gas will determine how much of each gas passes through the membrane, and hence will give us the selectivity of the membrane for either of the gases.

Gas Chromatography is a general term used for that type of chromatography, in which the mobile phase is a gas. Gas Chromatography is carried out in an apparatus called Gas Chromatograph. A typical Gas Chromatograph consists of the following pieces of equipment:

- Carrier gas tank
- Sample injection port
- GC column
- Detector
- Attenuator
- Chart recorder

The carrier gas is fed into the sample injection port, where our test gas samples are also kept. Both the carrier gas and the feed gas are mixed, and introduced into the gas chromatography column. The column is filled with the stationary phase, which interacts differently with different components of the feed whereas the carrier gas does not interact with the stationary phase. At the end of the column is a detector, that measures the amount of each gas exiting the column. The column is kept at elevated temperatures, to keep the

sample in vapor phase. The output of the detector is then converted into interpretable data by an attenuator, then displayed as a graph called a chromatogram.

For mixed gas permeation and separation testing, Perkin-Elmer Clarus 580 Chromatograph is used. CO_2/CH_4 (10:90 by volume) gas mixture is used as the feed gas for this purpose, which passes through the membrane. The gas feed into the column and permeate that has passed through the membrane. The testing is carried out at different pressures, just like in the case of single gas permeation testing. The test pressure ranged from 1 bar to 5 bars pressure. Thus, we found the amount of CO2 and CH4 on the permeate side, using the results from this test, which come out in the form of a chromatogram[115].

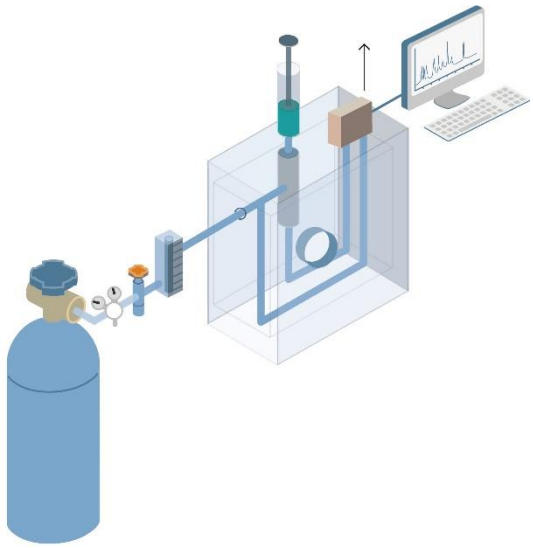

[116] Figure 13: schematic diagram of gas chromatography

Chapter 4

Results and discussion

4.1 Characterization technique

Different characterization techniques have been used to analyze the membranes for their different properties. The various techniques used for characterization are as follows:

- Fourier Transform Infra-Red (FT-IR) Spectroscopy, qualitatively examine the different functional groups within the membrane structure.
- Scanning Electron Microscopy, used to analyze surface morphology and pore characteristics of the membrane.
- Tensile testing analysis, used to test the mechanical strength of the membranes.
- X-ray diffraction, used to verify the presence of crystallinity in filler and polymeric membrane matrix.

4.2 FTIR Spectroscopy Analysis

4.2.1 FTIR of pure γ-CD-MOF, PU and PU/γ-CD-MOF mixed matrix membrane

Now FTIR graph of γ-CD-MOF, pure polyurethane and PU/γ-CD-MOF in figure 14. The qualitative analysis between polymer and filler is explained by FTIR spectroscopy in fig. 14. The graph showed the FTIR of γ-CD-MOF, pure PU and PU/γ-CD-MOF mixed matrix membrane. In case of γ-CD-MOF major peak of concern is hydroxyl peak (-OH) appeared at 3390 cm^{-1} as proper bell shaped peak. In addition, second major peak is of $–CH_2$ group prominent at 2928 cm^{-1}. Another promising peak of C-O-C in γ-CD-MOF thought to appear around 1027-1157 cm^{-1}[117].

In case of pure polyurethane membrane very complex FTIR spectroscopy given in figure. As PU is a co-polymer and composed of urethane hard segment (-R-O-CO-NH-R-) and ether soft segments (-C-O-C-). The major peak is amine peak N-H stretching appeared at 3449.55 cm^{-1}, this amine peak in graph also called shoulder peak due to its appearance. Generally amine peak is a part of hard segment in PU and presence of carbonyl group C=O is of soft segment appeared at 1698.46 cm^{-1}. The two main peak of PU $–CH_2$ stretching ($–CH_2$ peak range is 2500-3000cm^{-1}) and ether C-O-C representing by graph at

2931cm^{-1} and 1112cm^{-1} respectively. A very narrow bell shaped peak of hydroxyl group –OH due to presence of polyether polyols group also showed at 3327.91cm^{-1} and normally its range is 2400-3600cm^{-1}. Spectrum of N-H stretching region gives idea about the degree of hydrogen bonding of N-H group, with adjacent carbonyl group C=O. therefore, in respect of pure polyurethane membrane, intermolecular interaction of carbonyl group and amine group in hard segment (N-H…….O=$C_{urethane}$) at 3327cm^{-1}[101, 103].

In case of PU/γ-CD-MOF membrane no significant shift or disappearance of peaks observed as compared to pure PU and γ-CD-MOF peaks. Rather trivial decrease in magnitude of peak observed in case of PU/γ-CD-MOF. Amine group N-H in hard segment through hydrogen bonding link with carbonyl group C=O of soft segment (N-H…….O=C_{ether}). Amine peak appeared in the form of shoulder peak at 3449 cm^{-1} also justify its presence. With the incorporation of filler in PU matrix peak intensity of amine group reduced as compared to pure PU membrane. This drop is due to phase separation take place between PU and γ-CD-MOF filler. As –OH peak appeared at 3327.91cm^{-1} in pure PU and around 3390cm^{-1} of γ-CD-MOF, hence in PU/ γ-CD-MOF MMM it appeared at 3330cm^{-1} justified the physical interaction polymer with filler. Due to incorporation of γ-CD-MOF in PU no permanently disappearance of peak observed, only slight shifting of peaks witnessed. As –CH_2 peak now noticed at 2939cm^{-1} in PU/γ-CD-MOF membrane, similarly amine (N-H) and carbonyl group (C=O) also exhibited very slight shift i.e. at 3449cm^{-1} and 1702cm^{-1} respectively[98, 100].

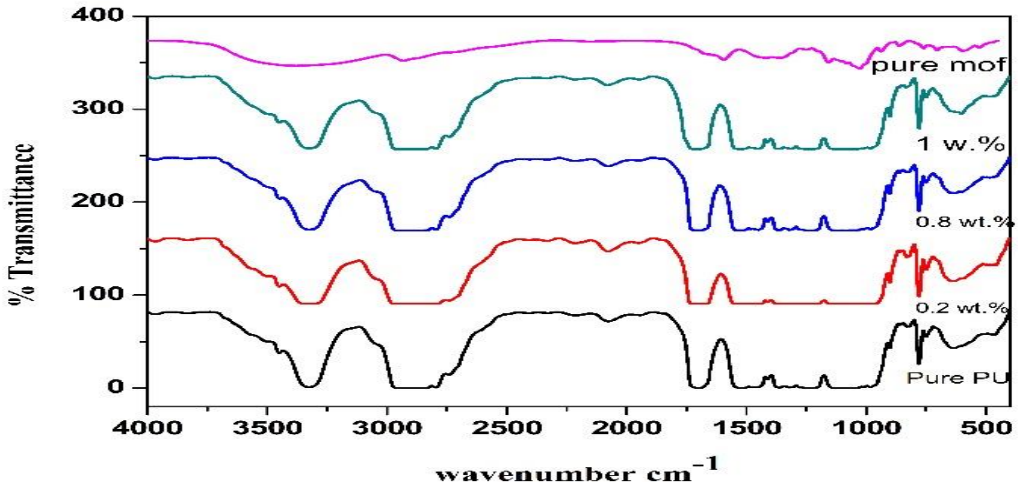

Figure 14: FTIR of pure PU, γ-cd-mof and PU/γ-cd-mof

4.2.2 FTIR of pure γ-CD-MOF, CA and CA/γ-CD-MOF mixed matrix membrane

As shown in Figure 15, the presence of different functional groups is confirmed by analyzing the pure CA, CA/γ-CD-MOF membrane and γ-CD-MOF samples using FT-IR spectroscopy. Firstly, we have the spectrum of the membrane sample made of pure CA. It contains a perfectly bell-shaped inverted peak at the wavenumber value of 3487 cm^{-1}, which is due to the stretching vibrations of the O-H bond. Moving on, we see a sharp peak at 2965 cm^{-1}, signifying the presence of Csp_3-H bond. Lastly, we see a peak at 1741.95 cm-1, thereby confirming the presence of C=O bond. Furthermore, at 1640cm^{-1} bending vibration mode of molecular water is more prominent, 1375cm^{-1} representing $–CH_3$ symmetric deformation stretching and at 1241cm^{-1} represents the C-C-O acetate group stretching[106, 118].

In case of CA/γ-CD-MOF 0.2 wt. % major peaks of concerned are hydroxyl group (-OH) peak which is common in both of polymer and filler. So, in hybrid of polymer and filler this inverted bell shaped peak become narrow and appeared at 3489cm^{-1} in perfect agreement between mof and polymer individual peaks. Although, because of overlapping of hydroxyl peak of both polymer and filler its intensity appeared to be increased. Next major peak of concerned is of $–CH_2$ group peak of γ-CD-MOF noticed at 2928cm^{-1} and $–CH_3$ ($-C_{sp3}$-H) peak of CA at 2965cm^{-1}, in CA/γ-CD-MOF membrane both former peaks merger together and an intermediate peak observed at 2945cm^{-1}. At this point it's difficult to declare which functional group it is representing by this peak either of $–CH_2$ or $–CH_3$. At 1027-1157cm^{-1} stretching vibration mode of C-O-C appeared of γ-CD-MOF. More ever stretching vibration peak of C-O bridge of CA witnessed at 1150cm^{-1}, now in case of CA/γ-CD-MOF mixed matrix membrane due to interaction between C-O-C group and C-O series of peaks appeared in between 1053-1160cm^{-1}. By concluding the FTIR spectrometry analysis, it was being appeared that no chemical interaction take place between CA and γ-CD-MOF after their fabrication in CA/γ-CD-MOF mixed matrix membrane, only physical bonding exists between CA and γ-CD-MOF[93, 119].

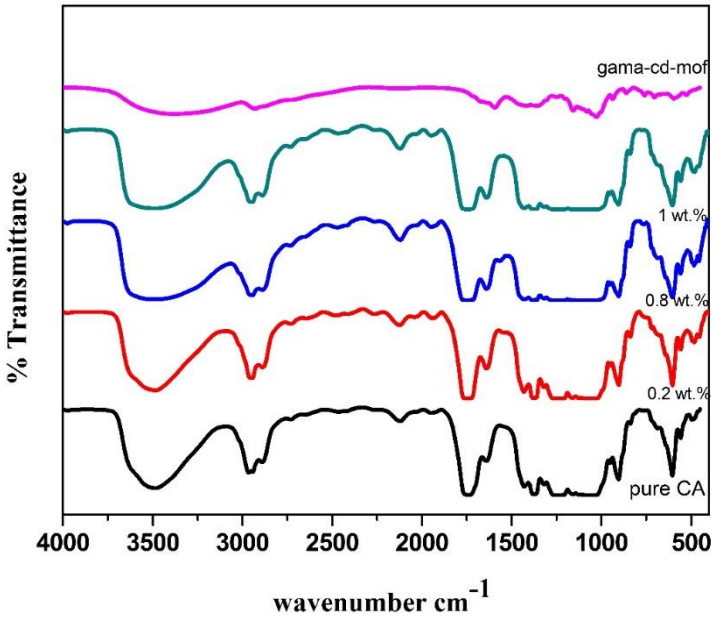

Figure 15: FTIR of pure mof, pure CA, CA/0.2 wt. %, CA/0.8 wt. %, CA/1

4.3 Ultimate tensile strength of pure and mixed matrix membrane

4.3.1 Mechanical properties of pure PU and PU/γ-CD-MOF MMM

Mechanical properties of both pure and hybrid membrane can be measured by ultimate tensile machine and results are displayed in bar graphs in fig. 16.

As shown in Figure 16, the mechanical stability of various samples of pure and PU/γ-CD-MOF MMM measured at an elongation rate of 10 mm/min. This value of elongation is picked after several runs with both high and low elongation rates ranging from 0.1 to 10mm/min. When the elongation rate is too low, the tensile strength is much higher than it should be; whereas if the elongation rate is too high, the tensile strength is much lower than expected. Only, at a moderate value of elongation rate such as 10 mm/min, will the membrane strength be more accurately represented.

Pure polyurethane membrane can resist stress up to 21.87MPa before it finally breaks, and by increasing filler concentration from 0.2 wt. % gradually to 1 wt. %. Almost regular trend observed in terms of increasing and decreasing of mechanical strength of pure and hybrid membrane. Now by incorporating γ-CD-MOF 0.2 wt. % in PU increase in mechanical strength observed for hybrid membrane but its magnitude is less than that of

pure PU. From o.2-o.6 wt. % addition of filler in PU increase in mechanical strength observed for PU/γ-CD-MOF hybrid membrane. Due to addition of mod in polymer no aggregation of filler particle observed on surface or in cross-section of polymer. And no voids or gaps appeared due to filler assimilation in polymer, this result in increase in mechanical strength of membrane. The phenomena involved is the developing of hydrogen bonding between hydroxyl group (-OH) in γ-CD-MOF with amine group (N-H) in hard segment of PU. Similarly, hydroxyl group in polyols also develop strong affinity with –OH group of filler due to dipole-dipole or hydrogen bonding and provide significant high mechanical strength and strain rate in PU/γ-CD-MOF hybrid membrane. And further increasing filler concentration 0.8-1 wt. % a sudden decline in mechanical strength experienced in membrane sample. This drop in strength of membrane sample due to increase in polymer-filler interfacial area, which developed weak polymer-filler junction and also restricted the mobility of polymer chain in this area. In addition, rigidity or brittleness also introduced in weak polymer-filler junctions that contribute in decline of mechanical strength[101, 102].

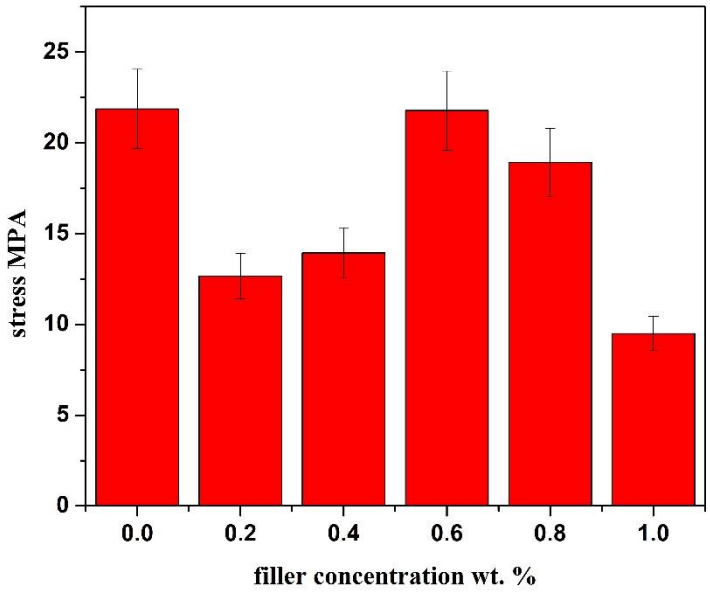

Figure 16: tensile strength of pure PU and PU/γ-cd-mof 0.2-1 wt. %

4.3.2 Mechanical properties of pure CA and CA/γ-CD-MOF MMM

As shown in Figure 17, the mechanical stability of various samples of pure and CA/γ-CD-MOF MMM measured at an elongation rate of 0.5 mm/min. Table 5 also represented the detail of elongation rate and tensile strength of all samples. Pure cellulose acetate membrane can undergo maximum stress up to 4.6MPa due to not having proper orientation of polymeric chain and presence of micro voids between chains that halted polymeric chain to orient in proper symmetry, hence it resulted in reduction of mechanical strength. By the incorporation of γ-CD-MOF (filler) in cellulose acetate matrix considerably increase in mechanical strength observed. Tensile strength and young modulus of MMM increased when γ-CD-MOF concentration increased from 0.2 wt. % to 1 wt. %. It's due to better dispersion and interfacial interaction between γ-CD-MOF and cellulose acetate. Gradual increasing trend in tensile strength of CA/γ-CD-MOF MMM also support the absence of any agglomeration of filler particle in polymeric matrix. As agglomeration caused drop in tensile strength of membrane because of presence of weak domains developed in polymeric chains[120].

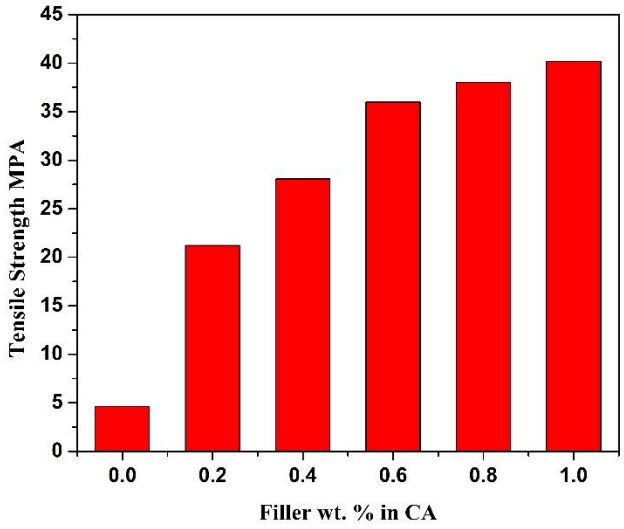

Figure 17: Tensile strength of pure CA and CA/γ-cd-mof 0.2-1 wt. %

Table 6: Tensile stress of pure CA and CA/γ-cd-mof 0.2-1 wt. %

Membrane sample	Percentage Elongation	Tensile stress MPA
Pure CA		
CA/γ-CD-MOF 0.2 wt.%	21.150	21.22
CA/γ-CD-MOF 0.4 wt.%	4.65	28.61
CA/γ-CD-MOF 0.6 wt.%	5.956	36
CA/γ-CD-MOF 0.8 wt.%	8.35	38
CA/γ-CD-MOF 1 wt.%	4.22	40

4.4 X-Ray Diffraction of pure and Mixed Matrix Membrane

4.4.1 XRD analysis of pure PU, γ-CD-MOF and PU/γ-CD-MOF MMM

Figure 18 shows the x-ray diffraction graph of pure PU, γ-CD-MOF and PU/γ-CD-MOF MMM. Pure PU membrane showed broad peak at $2\theta=20^0$. This major peak might be due to the existence of infinitesimal crystalline region of one of basic precursor of polyurethane i.e. polytetra methylene glycol (PTMG). In addition, another main peak seen in graph at $2\theta=23^0$ in PU/γ-CD-MOF because of crystallinity of hard segment of polyurethane. Integration of nano-particles, zif, zeolites etc. in PU result in decreasing its crystallinity, but incorporation of γ-CD-MOF retained its crystalline nature. As γ-CD-MOF also have body centered cubic structure and retained its crystalline nature after integrating in polymeric matrix, also justify by SEM images [60, 102, 121].

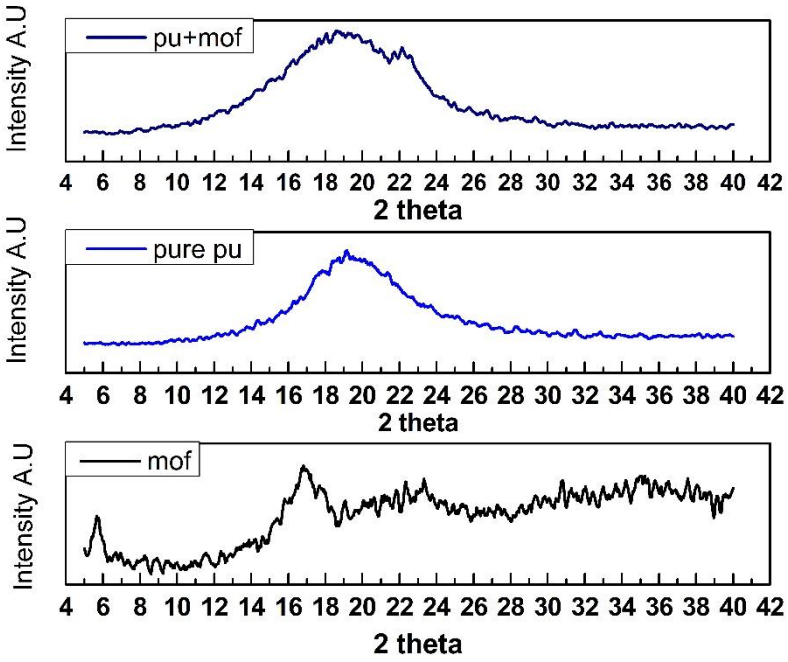

Figure 18: XRD of (a) pure mof, pure PU and PU/γ-cd-mof (b) pure PU and PU/γ-cd-mof

4.4.2 XRD analysis of pure CA, γ-CD-MOF and CA/γ-CD-MOF MMM

Figure 19 shows the x-ray diffraction pattern of pure CA membrane, CA/γ-CD-MOF MMM and pure γ-CD-MOF (filler). Γ-CD-MOF have body centered cubic crystal geometry and dominant diffraction peak mostly appeared at $2\theta=6^0$, $2\theta=13^0$, $2\theta=17^0$, $2\theta=23.5^0$. More prominent peak of γ-CD-MOF in range of 14^0 to 17^0 of KOH, K^{+1} cation coordinated with cyclodextrin ligand. CA membrane x-ray diffraction pattern reveal more amorphous structure with absence of sharp and prominent peak from 5^0 to 40^0. Rather characteristics peak as reported in many literature correspond to pure cellulose acetate membrane is between $2\theta=17^0$ to $2\theta=19^0$.

In case of CA/γ-CD-MOF MMM hybrid formed between polymer and filler. Major peaks of both cellulose acetate and γ-CD-MOF are observed in CA/γ-CD-MOF hybrid x-ray diffraction pattern. But the magnitude of major peaks of γ-CD-MOF decline because of its very less concentration in polymeric matrix. Nevertheless, γ-CD-MOF retained its crystalline structure even after its incorporation in polymeric matrix, and also seen in SEM images the bcc geometry of γ-CD-MOF after its immersing in CA matrix [66, 122, 123].

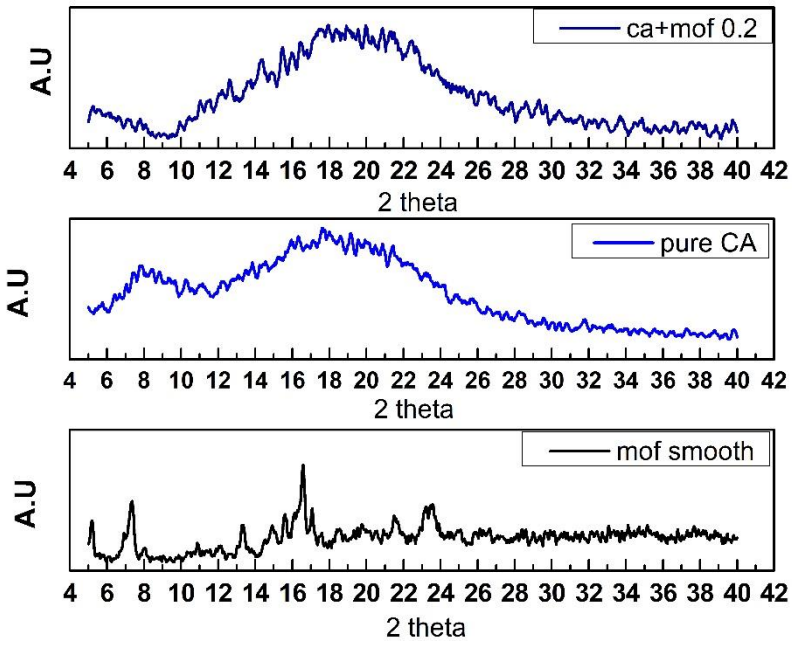

Figure 19: XRD of pure CA, CA/γ-CD-MOF and pure γ-CD-MOF

4.5 Scanning electron microscopy analysis of membranes

4.5.1 SEM analysis of pure PU and PU/γ-CD-MOF mixed matrix membrane

SEM images of pure PU and PU/γ-CD-MOF MMM are shown in figure 20-25 of pure PU and PU/γ-CD-MOF 0.2, 0.4, 0.6, 0.8 and 1 wt. % respectively. On different magnification of 5000x, 10,000x, 20,000x and 25000x SEM images had been taken and best and most optimize images were selected for detail description. At 10,000x magnification and accelerating voltage of 5kV pure PU membrane show highly dense surface morphology, free from any voids, pores or any uneven surface area. In figure 21 PU/γ-CD-MOF 0.2 wt. % membrane sample highly dense surface layer seen and no agglomeration of filler observed on the surface of polymeric matrix. From figures 22 to 25 as filler concentration increase from 0.4 wt. % to 1 wt. % all hybrid sample surface is highly compact and dense. No micro voids or any cavities were seen in any sample and no coalescence of filler particles observed. Rather γ-CD-MOF retained its body-centered cubic structure even

after it immersed in polymeric matrix. This retention of its crystalline structure strengthened the assumption of physiosorption phenomena taking place during gas flow through PU/γ-CD-MOF MMM. Due to continuous feed supply γ-CD-MOF adsorb carbon dioxide from mixture of gas because of affinity with CO_2 molecule and allow it to permeate through PU/γ-CD-MOF MMM, but retain the flow of methane CH_4 gas. And furthermore, due to continuous feed supply and difference of pressure on feed and permeate side physically adsorb CO_2 molecule by γ-CD-MOF detached and permeate from membrane and active site become available for upcoming CO_2 molecule, hence this process continues and CO_2 separates from methane from feed stream.

At 1 wt. % PU/γ-CD-MOF membrane sample no pores generated in membrane and no agglomeration of filler observed, hence forth, no sharp increase in permeability of both CO_2 and CH_4 occurred rather significant increase in selectivity of CO_2/CH_4 observed[121, 124, 125].

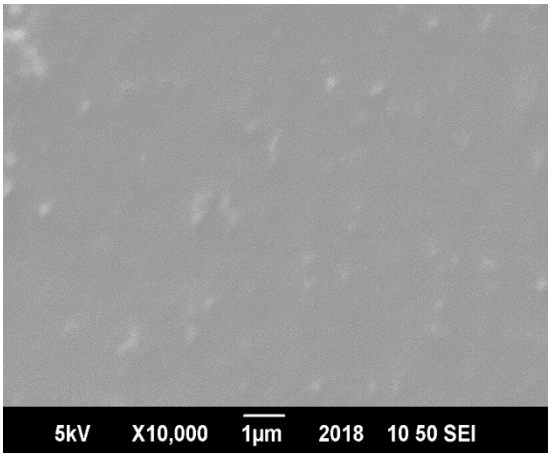

Figure 20 : Pure Polyurethane membrane

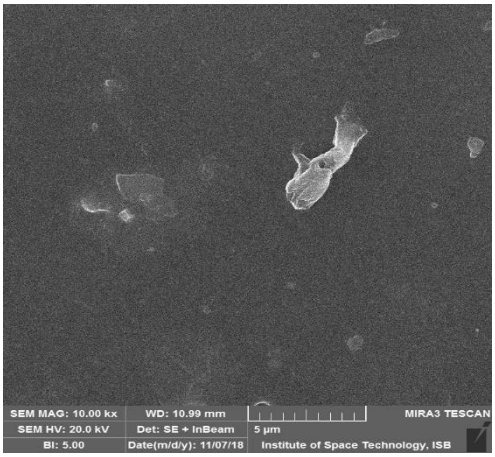

Figure 21: PU/γ-cd-mof 0.2 wt. %

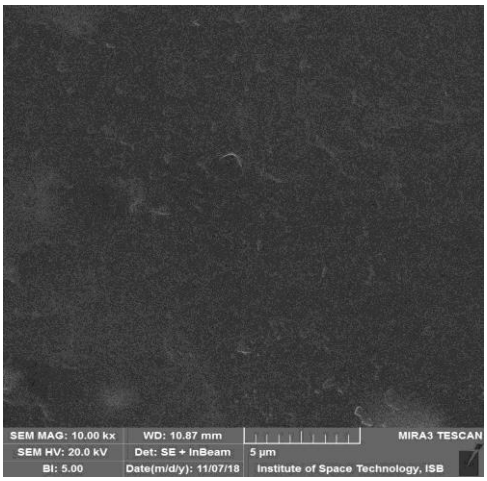

Figure 22: PU/γ-cd-mof o.4 wt. %

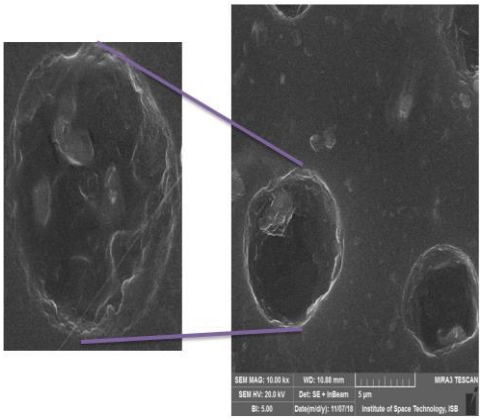

Figure 23: PU/γ-CD-MOF 0.6 wt%

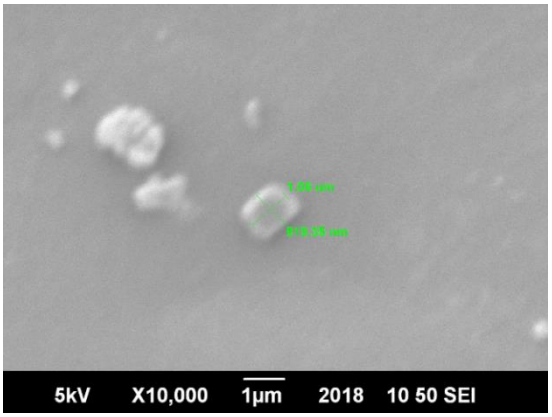

Figure 24 : PU/γ-CD-MOF 0.8wt. %

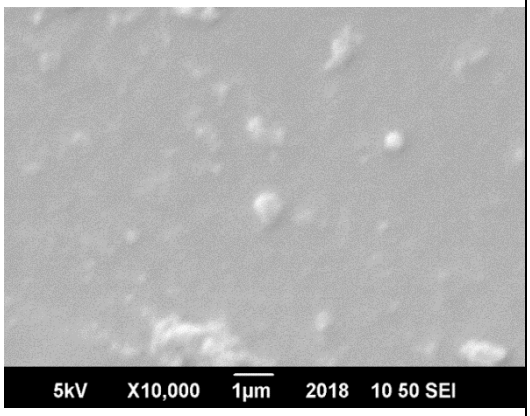

Figure 25: PU/γ-cd-mof 1 wt. %

Cross section images of PU/γ-CD-MOF of 0.2 wt. %, 0.4 wt. % and 0.6 wt. % hybrid membranes in figure 26, 27 and 28 (a) and (b) respectively revealed no micro voids or pores in any samples. In addition, measured thickness is equal to membrane thickness measured manually using screw gauge. This images justify the solution-diffusion model employed for the permeation of gas through membrane[126].

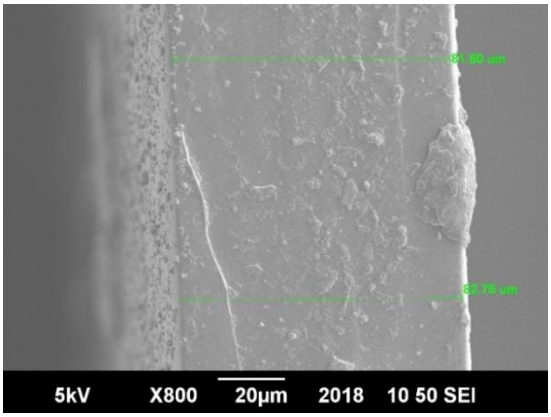

Figure 26: Cross section of PU/γ-CD-MOF 0.2 wt.%

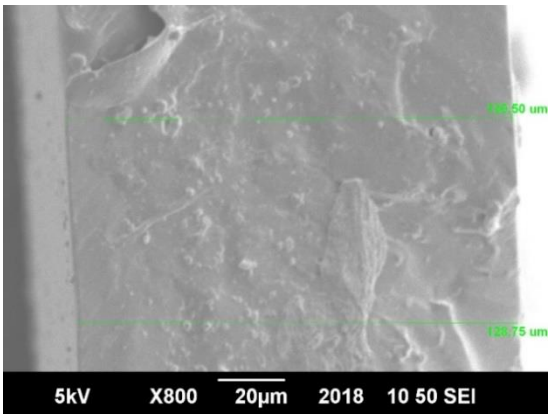

Figure 27: cross section of PU/γ-CD-MOF 0.4 wt. %

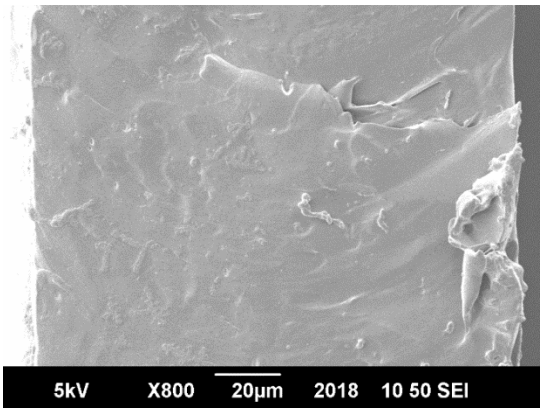

Figure 28(a): cross section of PU/γ-CD-MOF 0.6 wt. %

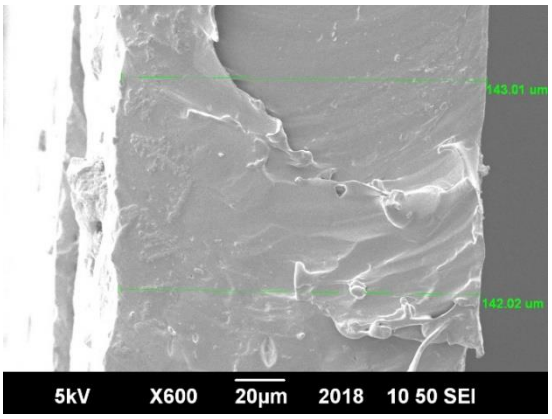

Figure 28(b): cross section of PU/γ-CD-MOF 0.6 wt. %

4.5.2 SEM analysis of pure CA and CA/γ-CD-MOF mixed matrix membrane

SEM images of pure cellulose acetate membrane and CA/γ-CD-MOF mixed matrix membrane of their surface as shown in figure 29 (a), (b) (c), (d), (e) and (f). Figure 29 (a) shows the smooth surface of CA membrane with dense surface morphology of polymeric chains to membrane/air interface. Absence of any voids or pores in pure CA membrane is also due to uniform evaporation of solvent which allow polymeric chains to arrange in regular pattern and reduced any void formation. When γ-CD-MOF integrate into CA, CA/γ-CD-MOF mixed matrix membrane have average membrane thickness 60µm and have denser layer. In fig. 29 (b) CA/γ-CD-MOF 0.2wt. % the filler is uniformly dispersed on polymeric matrix because of co-sonication before casting. As it clearly seen in SEM images, γ-CD-MOF crystals also retained their body centered cubic crystal geometry even

after immersing in polymeric matrix. As filler concentration increases from 0.4 to 1 wt. % CA/γ-CD-MOF membrane morphology remain dense and no voids or pores appeared on surface. But as concentration of filler increased membrane surface become rough and in higher concentrations, agglomeration of filler also seen in CA/γ-CD-MOF 1wt. % sample. The agglomeration of γ-CD-MOF within the CA polymeric matrix was due to van der Waal forces and hydrogen bonding between hydroxyl groups among γ-CD-MOF molecules. As both cellulose acetate and γ-CD-MOF are hydrophilic in nature and denatured by exposing in moisture or interaction with water. So CA/γ-CD-MOF membrane should be employed where there is no moisture content available [127, 128].

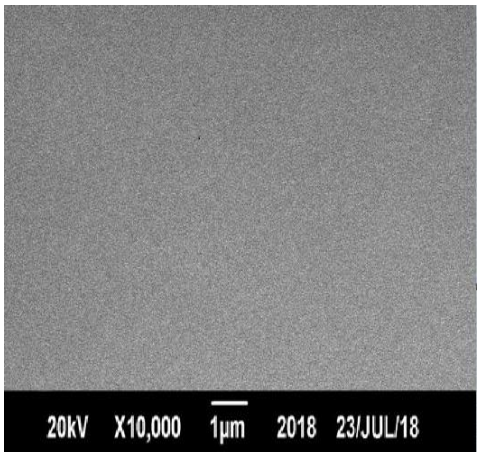

Figure 29(a): pure CA

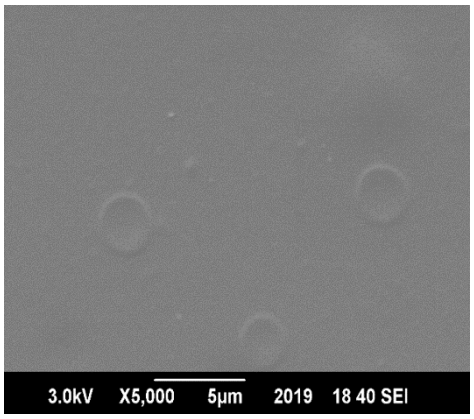

Figure 29(b): CA/MOF 0.2 wt. %

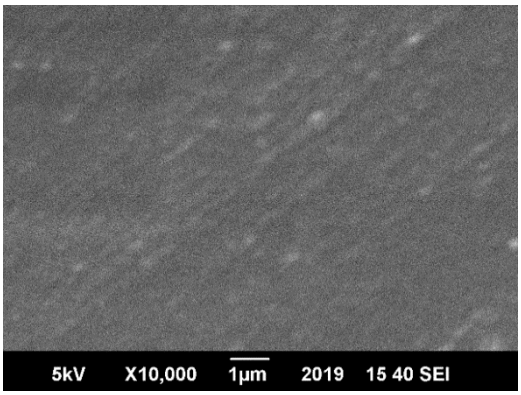

Figure 29(c): CA/γ-CD-MOF0.4wt. %

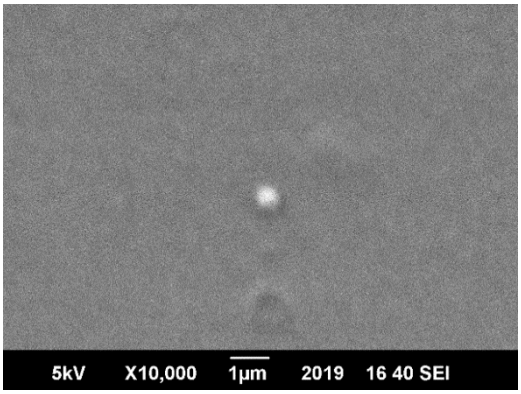

Figure 29(d): CA/γ-CD-MOF0.6wt. %

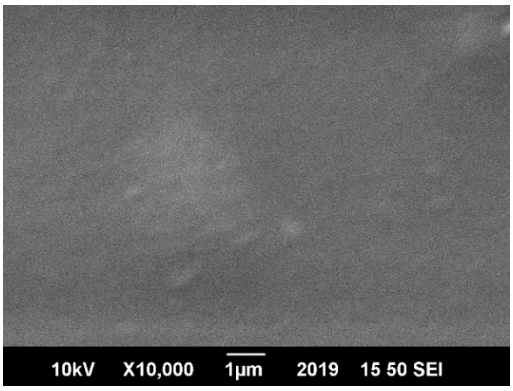

Figure 29(e): CA/γ-CD-MOF 0.8 wt. %

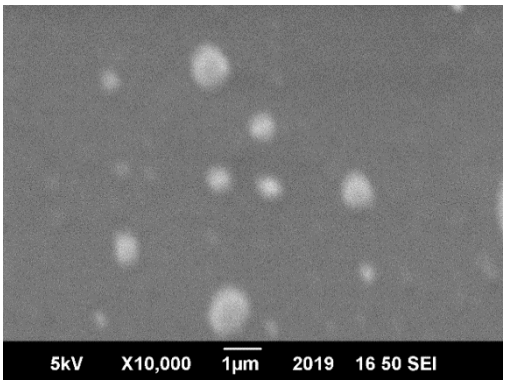

Figure 29(f): CA/γ-CD-MOF 1 wt. %

4.6 Gas permeation testing

4.6.1 Single gas testing of Pure PU and PU/γ-CD-MOF MMM

Single gas permeation testing was carried out for pure polyurethane and PU/γ-CD-MOF mixed matrix membranes containing 0.2%, 0.4%, 0.6%, 0.8% and 1% γ-CD-MOF in PU membranes. The permeation testing was carried out in the PHILOS Gas Permeability Testing System fitted with a gas permeation rig. The permeability of CO_2 and CH_4 through

the membranes were calculated at pressure values of 1-5 bar and corresponding selectivity were also calculated, as shown in Table 7.

Table 7: single gas testing of pure PU and PU/γ-CD-MOF membrane samples

Membrane	**Permeability CO_2 barrer**	**Permeability CH_4 barrer**	**Selectivity CO_2/CH_4**	**Pressure bar**
Pure PU	270	38	07	01
Pure PU	198	18	11	02
Pure PU	167	14	12	03
Pure PU	166	12	14	04
Pure PU	112	5	21	05
PU/γ-CD-MOF 0.2 wt.%	371	16.07	23.08	01
PU/γ-CD-MOF 0.2 wt.%	287	11.38	25.20	02
PU/γ-CD-MOF 0.2 wt.%	235	8.92	26.34	03
PU/γ-CD-MOF 0.2 wt.%	219	7.97	27.46	04
PU/γ-CD-MOF 0.2 wt.%	214	7.49	28.56	05
PU/γ-CD-MOF 0.4 wt.%	470	24.73	19	01
PU/γ-CD-MOF 0.4 wt.%	228	11	20.12	02
PU/γ-CD-MOF 0.4 wt.%	217	10	21.24	03
PU/γ-CD-MOF 0.4 wt.%	195	8.6	22.48	04
PU/γ-CD-MOF 0.4 wt.%	186	8.0	23.02	05
PU/γ-CD-MOF 0.6wt. %	262.32	15	16.66	01
PU/γ-CD-MOF 0.6 wt.%	195	11	17.01	02
PU/γ-CD-MOF 0.6 wt.%	186.08	10	17.54	03
PU/γ-CD-MOF 0.6 wt.%	168	09	18.84	04
PU/γ-CD-MOF 0.6 wt.%	161.43	08	19.01	05

PU/γ-CD-MOF 0.8 wt. %	181	16.45	11	01
PU/γ-CD-MOF 0.8 wt. %	163	12.53	13	02
PU/γ-CD-MOF 0.8 wt. %	111	7.4	15	03
PU/γ-CD-MOF 0.8 wt. %	69	3.52	19.56	04
PU/γ-CD-MOF 0.8 wt. %	70	2.9	24	05
PU/γ-CD-MOF 1 wt. %	50	10	05	01
PU/γ-CD-MOF 1 wt. %	42	6.46	6.5	02
PU/γ-CD-MOF 1 wt. %	35	05	07	03
PU/γ-CD-MOF 1 wt. %	29	03	9.6	04
PU/γ-CD-MOF 1 wt. %	26	1.2	21	05

4.6.1.1 Effect of filler concentration on CO_2 and CH_4 permeability

The permeability and selectivity of CO_2 and CH_4 demonstrated by both linear and bar graph with different parameters. Initially graph was plotted between filler concentration and permeability for CO_2 and CH_4. In fig. 30 graph shows decrease in permeability of both CO_2 and CH_4 with increasing filler concentration in PU/γ-CD-MOF mixed matrix membrane. These result were obtained at 5 bar pressure at $25C^0$ temperature. Neat PU showed permeability of CO_2 112 barrer and it increase with PU/γ-CD-MOF 0.2 wt. %. And with further addition of filler from 0.4 to 1wt. % a gradual drop off in permeability observed for CO_2. The reduction in permeability might be due to obstacles created by the presence of filler particles as it increased the diffusion path length. Polyurethane is composed of hard and soft segment and latter is responsible for permeating gas molecule. As mentioned in literature different nano-particles were dispersed mainly in soft segment of polyurethane and responsible for decrement in gas permeability. Similarly the assimilation of γ-CD-MOF in PU also caused decline in gas permeability, because it restricts the chain mobility and also hindered the movement of large molecule i.e. methane of kinetic diameter 3.80A [102, 129].

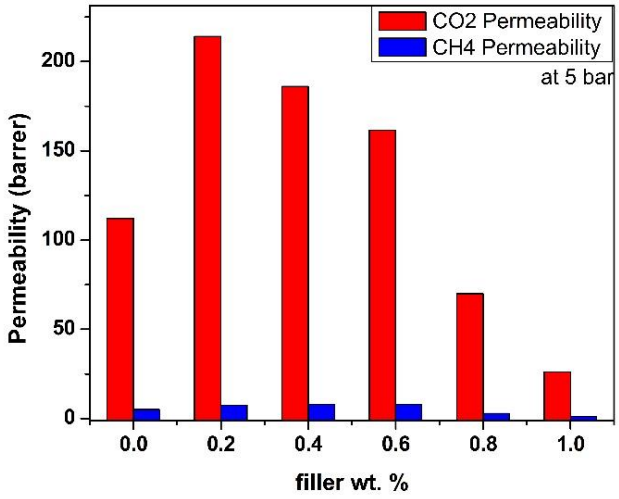

Figure 30: trend of filler wt. % on CO_2 and CH_4 permeability

4.6.1.2 Effect of feed pressure on permeability of gases in PU and PU/γ-CD-MOF MMM

Figure 31(a) represents the relation between pressure and permeability of CO_2 and CH_4 with respect to different weight percentage of filler in PU matrix. In all sample with increasing pressure from 1 to 5 bar permeability reduced. Maximum permeability achieved of CO_2 with PU/γ-CD-MOF 0.4wt. % sample and maximum selectivity achieved for CO_2/CH_4 with PU/γ-CD-MOF 0.2wt. % sample. Also mentioned in above paragraph the filler prefer to distribute in soft segment of polyurethane. And it might be the possibility of developing van der Waal interaction between hydroxyl groups –OH of γ-CD-MOF with ether group of soft segment in PU. So when the weight percent of γ-CD-MOF increase it adsorb more carbon dioxide molecule and increase the diffusion path length for gases and retained the permeation of molecule having high kinetic diameter e.g. methane. In addition, larger gas molecule are more constrained in crossing polymer chains thickness than smaller ones and large reduction in permeability observed for CH_4 in comparison with CO_2. Moreover, due to presence of amine group N-H and hydroxyl group in PU and also large number of –OH groups in single γ-CD-MOF molecule have developed more affinity towards carbon dioxide as compared to methane. Hence, it resulted in achieving better values of selectivity for CO_2/CH_4 especially at high pressure i.e. 5 bar in all PU/γ-CD-MOF hybrid samples.

It's been assumed that solution-mechanism model and Henry's Law of sorption would better explain the permeation of gases through PU/γ-CD-MOF mixed matrix membrane. Further the free the presence of free volume in rubbery portion of polyurethane are responsible for the permeation of carbon dioxide as it permeates more than methane.

Total sorption in glassy polymer is:

$C_m = C_D + C_H$

In case of permeation through free volume:

$C_D = K_D p$

In case of permeation through excess free volume:

$C_H = \frac{C_H + bp}{1 + bp}$

Total:

$C_m = K_D p + \frac{C_H + bp}{1 + bp}$

Similarly figure 31(b) demonstrates the decrease in permeability of methane with increase in concentration of filler at 5 bar pressure. A similar trend to that of carbon dioxide observed in this graphs, but permeability of methane is too much low. Because of large kinetic diameter 3.80A and having non-polar nature, no affinity develop with functional group presents in PU/γ-CD-MOF membrane. Also it can be explained by the fact that there may be a more tortuous path for the gas molecules to travel to get to the permeate side, as the filler is increased. Moreover, as the amount of filler increases, the molecular chains of the polymer become less mobile and more rigid as more filler is added, which would hinder the permeability of gas molecule [60, 130-132].

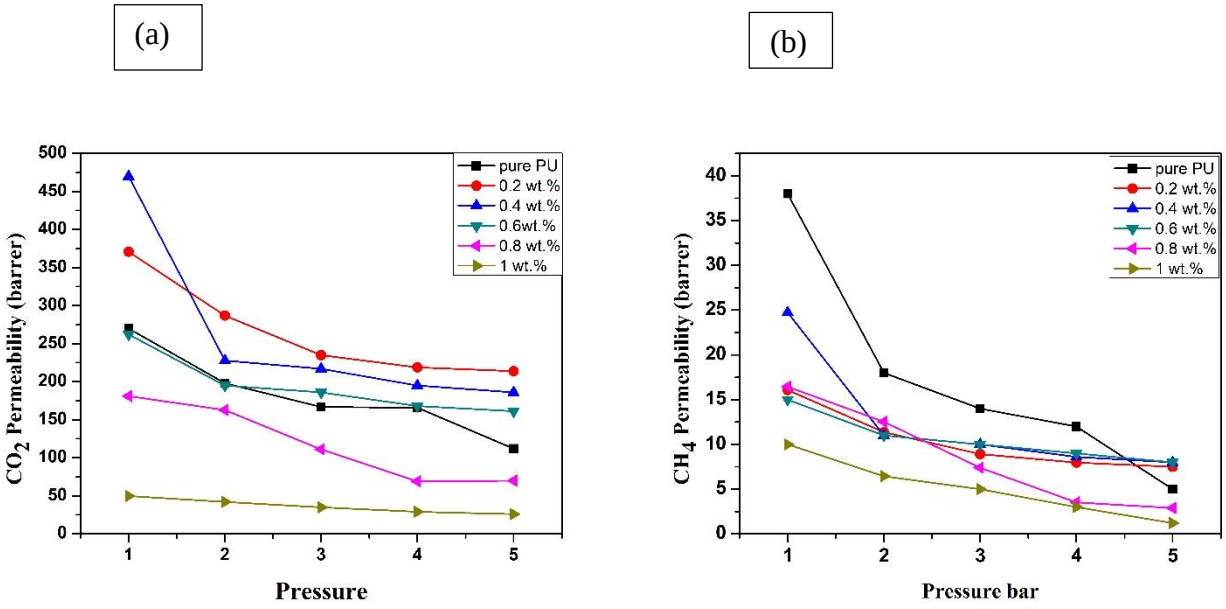

Figure 31: trend of pressure on (a) CO_2 permeability (b) CH_4 permeability

4.6.1.3 Relationship between selectivity of CO_2/CH_4 and feed pressure

A graph was plot between selectivity of CO_2/CH_4 vs pressure for pure PU and PU/γ-CD-MOF samples in figure 32. It can be seen clearly with the rise of pressure, selectivity of CO_2/CH_4 increased significantly. And maximum selectivity achieved at 5 bar pressure in all samples of membranes. Carbon dioxide permeate more preferentially as compared to methane, as CO_2 is more condensable than methane because of its small kinetic diameter 3.30A and also because of drop in rubber properties of polyurethane. This is due to less movement of polymeric chains due to incorporation of filler particles which restricts chain movement. Therefore, gas molecules of larger molecular size have to take more convoluted path for permeating through membrane. In contrast due to presence of –OH and amine N-H group affinity developed for carbon dioxide and it follows solution-mechanism model for permeating through membrane, first diffuse and then dissolve through the matrix and again diffuse on the permeate side of membrane[129].

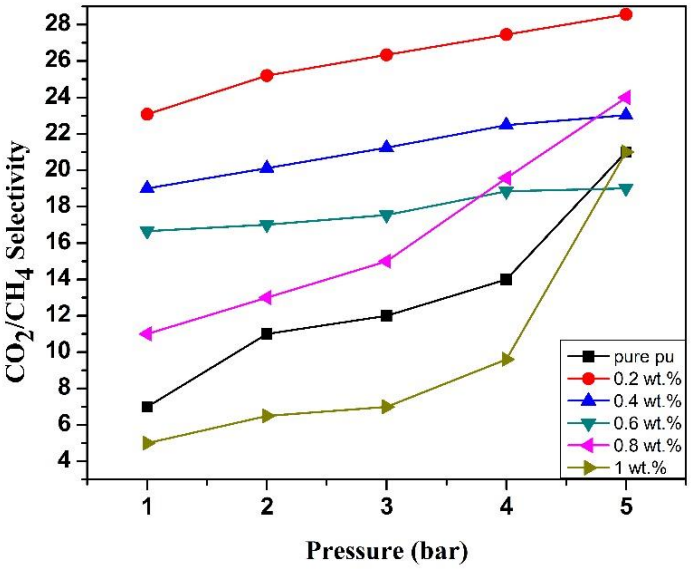

Figure 32: trend of CO_2/CH_4 selectivity with pressure

4.6.2 Mixed gas permeation testing for PU and PU/γ-CD-MOF MMM

For mixed gas permeation testing, we used CO_2/CH_4 mixture (50:50 by volume). Moreover, we used GC column for checking the composition of the mixture coming out of permeate of the membrane, and this will give us the selectivity of the pure Pu and PU/γ-CD-MOF mixed matrix membrane. The values for the gas permeability and the mixed gas selectivity can be shown in the tables 8.

Table 8: Permeation table for mixed gas testing for pure PU and PU/γ-CD-MOF MMM

Membrane	Permeability CO_2 barrer	Permeability CH_4 barrer	Selectivity CO_2/CH_4	Pressure bar
Pure PU	228	35	6.5	01
Pure PU	167	16	10.4	02
Pure PU	141	13	10.8	03
Pure PU	140	11	12.72	04
Pure PU	94	4.8	19.24	05
Pu+MOF 0.2 wt.%	313	14.8	21.15	01
Pu+MOF 0.2 wt.%	242	10.48	23.09	02
Pu+MOF 0.2 wt.%	198.76	8.23	24.13	03
Pu+MOF 0.2 wt.%	185.23	7.36	25.16	04
Pu+MOF 0.2 wt.%	181	6.91	26.17	05

Pu+MOF 0.4 wt.%	397.52	22.83	17.41	01
Pu+MOF 0.4 wt.%	192.84	10.46	18.43	02
Pu+MOF 0.4 wt.%	183.53	9.53	19.46	03
Pu+MOF 0.4 wt.%	165	8	20.60	04
Pu+MOF 0.4 wt.%	157.31	7.45	21.09	05
Pu+MOF 0.6wt. %	222	14.54	15.26	01
Pu+MOF 0.6 wt.%	165	10.59	15.58	02
Pu+MOF 0.6 wt.%	157.38	9.79	16.07	03
Pu+MOF 0.6 wt.%	142	8.35	17	04
Pu+MOF 0.6 wt.%	136.53	7.83	17.42	05
Pu+MOF 0.8 wt. %	153	15.3	10	01
Pu+MOF 0.8 wt. %	137.86	11.57	11.91	02
Pu+MOF 0.8 wt. %	94	6.84	13.74	03
Pu+MOF 0.8 wt. %	58	3.22	18	04
Pu+MOF 0.8 wt. %	59.20	2.69	22	05
Pu+MOF 1 wt. %	42.29	9.23	4.58	01
Pu+MOF 1 wt. %	35.52	5.92	6	02
Pu+MOF 1 wt. %	29.60	4.61	6.41	03
Pu+MOF 1 wt. %	24.52	2.78	8.8	04
Pu+MOF 1 wt. %	22	1.14	19.24	05

4.6.2.1 Effect of filler concentration on CO_2 and CH_4 permeability

Effect of filler loading on the permeability of CO_2 and CH_4 in mixed gas testing also showed similar trend to that of single gas testing in figure 33. When simultaneously mixture of CO_2/CH_4 strike on the surface of membrane CO_2 permeate easily while methane retains. Hence, CO_2 having smaller kinematic diameter show high permeability as compared to CH_4 having large kinematic diameter. Consequently, CO_2/CH_4 selectivity increase significantly [102, 133].

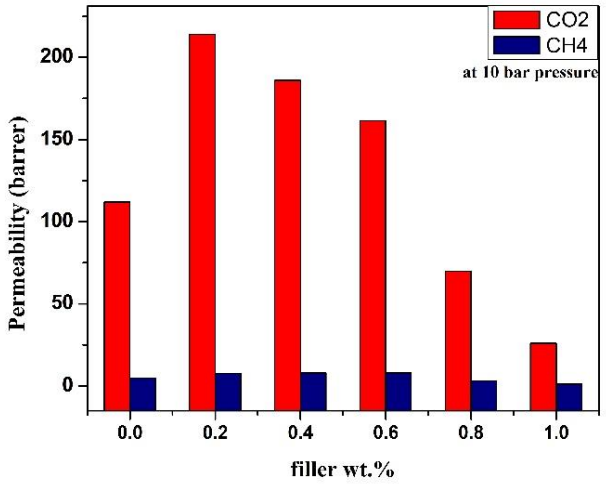

Figure 33: trend of filler wt. % on CO_2 and CH_4 permeability

4.6.2.2 Effect of feed pressure on gas permeability in mixed matrix membrane

Similarly to that of single gas permeation testing effect of feed pressure on the permeability of CO_2 and CH_4 through pure PU and PU/γ-CD-MOF membrane was examined and presented by graph in figure 34 (a) and (b). When mixture of CO_2 and CH_4 in 50% mole equilibrium concentration pass through pure PU and PU/γ-CD-MOF MMM, CO_2 permeates more as compared to CH_4. Phenomena involve in the gas transmission through PU/γ-CD-MOF membrane is solution-diffusion mechanism. Because of high condensability of CO_2, high solubility in PU matrix, small kinematic diameter 3.30A and polar nature that developed affinity with polar group present in PU chains and also with multiple –OH group present in γ-CD-MOF. It is assumed that the filler distributes in soft segment of PU and soft segments also responsible for permeation of gases. So, presence of γ-CD-MOF in soft segment reduce the available free volume between polymeric chain and restricting the gas diffusion path length. Thus, more tortuosity induced in the PU/γ-CD-MOF membrane matrix and it restricts the transmission of larger gas molecule i.e. CH_4 (3.80A) and permeability of smaller gas molecule CO_2 also reduced with increase in pressure [134-136].

(a) (b)

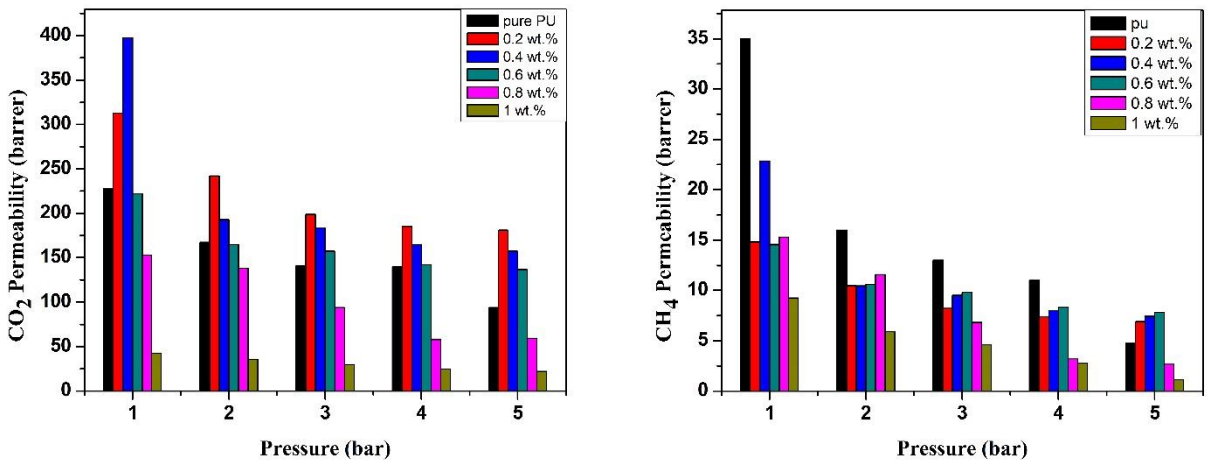

Figure 34: trend of pressure on (a) CO_2 permeability (b) CH_4 permeability with pressure

4.6.2.3 Effect of feed pressure on CO_2/CH_4 selectivity in pure PU and PU/γ-CD-MOF MMM

Figure 35 shows the effect of increasing pressure on the selectivity of CO_2/CH_4 through pure PU and PU/γ-Cd-MOF MMM. In mixed gas testing of equal volume of CO_2 and CH_4 (50:50) allowed to pass through pure PU and PU/γ-CD-MOF MMM. These results are similar to that of single gas testing and resulted in the decrease in permeability of both gases and increase in selectivity of CO_2/CH_4. When mixture of CO_2/CH_4 strike on the membrane surface, presence of abundant number of –OH group in γ-Cd-MOF and $-NH_2$ and –OH group in PU matrix develops more affinity with carbon dioxide as compared to methane. In addition, due to polar nature of CO_2 it dissolve into the polymeric matrix and diffuses while methane being non-polar not permeate with ease through PU/γ-CD-MOF membrane. Hence, permeability drops meaningfully for methane and selectivity of CO_2/CH_4 rise considerably [131, 137].

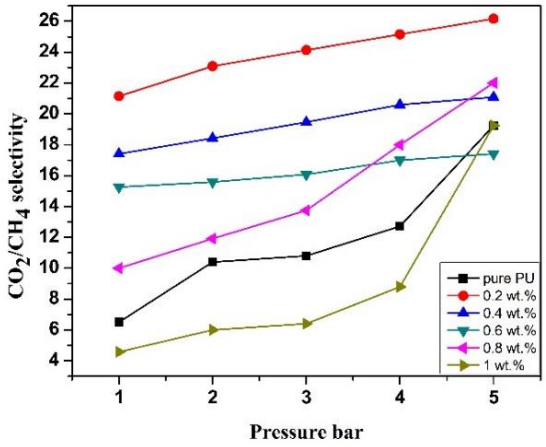

Figure 35: effect of pressure of selectivity of CO_2/CH_4

4.6.3 Gas permeation results of pure CA and CA/γ-CD-MOF MMM in single gas testing

Single gas permeation testing was carried out for pure CA and CA/γ-CD-MOF mixed matrix membranes containing 0.2%, 0.4%, 0.6%, 0.8% and 1% filler in CA membranes. The permeation testing was carried out in the PHILOS Gas Permeability Testing System fitted with a gas permeation rig. The permeability of CO_2 and CH_4 through the membranes were calculated at pressure 1-5 bar and corresponding CO_2/CH_4 selectivity were also calculated, as shown in Table 9.

Table 9: Permeation data for pure CA and CA/γ-CD-MOF in single gas testing

Membrane	**Permeability CO_2 barrer**	**Permeability CH_4 barrer**	**Selectivity CO_2/CH_4**	**Pressure bar**
Pure CA	30.09	15	2.0	1
Pure CA	23.75	14	1.6	2
Pure CA	23.14	13	1.78	3
Pure CA	20.75	11	1.8	4
Pure CA	19	10	1.9	5
CA+MOF 0.2 wt.%	64	2.065	31	1
CA+MOF 0.2 wt.%	42	1.313	32	2
CA+MOF 0.2 wt.%	40	1.212	33	3
CA+MOF 0.2 wt.%	24	0.686	35	4
CA+MOF 0.2 wt.%	18	0.489	36.79	5
CA+MOF 0.4 wt.%	34	1	34	1
CA+MOF 0.4 wt.%	26	0.742	35	2

CA+MOF 0.4 wt.%	22	0.602	36.5	3
CA+MOF 0.4 wt.%	20	0.540	37	4
CA+MOF 0.4 wt.%	17	0.441	38.49	5
CA+MOF 0.6 wt.%	23.14	0.701	33	1
CA+MOF 0.6 wt.%	16	0.471	34	2
CA+MOF 0.6 wt.%	15	0.422	35.55	3
CA+MOF 0.6 wt.%	12	0.333	36	4
CA+MOF 0.6 wt.%	15	0.405	37	5
CA+MOF 0.8 wt.%	28	0.875	32	1
CA+MOF 0.8 wt.%	21	0.636	33	2
CA+MOF 0.8 wt.%	17	0.500	34	3
CA+MOF 0.8 wt.%	16	0.451	35.5	4
CA+MOF 0.8 wt.%	13	0.361	36	5
CA+MOF 1 wt.%	39	1.258	31	1
CA+MOF 1 wt.%	29	0.906	32	2
CA+MOF 1 wt.%	24	0.727	33	3
CA+MOF 1 wt.%	23	0.676	34	4
CA+MOF 1 wt.%	12	0.343	35	5

4.6.3.1 Effect of filler concentration on gas permeability mixed matrix membrane

The permeability of both gases CO_2 and CH_4 in neat CA membrane higher than that of CA/γ-CD-MOF mixed matrix membrane. As shown in figure 36 and in table 10. The concentration of filler increase result in drop in permeability of both CO_2 and CH_4 at 5 bar pressure. These results are in perfect agreement with the Maxwell model. This model suggests there is decrease in gas diffusivity with increase in filler loading in mixed matrix membrane [107, 138]. Gamma-CD-MOF is potential substance for gas adsorption and that's why it is being incorporated into CA matrix for permeation study of gases. As its concentration increase the available free volume in CA is gradually filled by filler. The decrease in permeability of gases is due to the formation of agglomerates of filler in polymeric matrix, resulted in the development of non-selective voids in CA/γ-CD-MOF mixed matrix membrane.

Table 10: Effect of filler loading on CO_2/CH_4 selectivity in single gas testing.

Polymer-γ-CD-MOF loading	Permeability (barrer) CO_2	Permeability (barrer) CH_4	CO_2/CH_4 selectivity
CA-γ-CD-MOF-0%	19	10	1.9
CA-γ-CD-MOF-0.2 wt.%	18	0.489	36.79
CA-γ-CD-MOF-0.4 wt.%	17	0.441	38.49
CA-γ-CD-MOF-0.6 wt.%	15	0.405	37
CA-γ-CD-MOF-0.8 wt.%	16	0.361	35.5
CA-γ-CD-MOF-1 wt. %	12	0.343	35

There is physical interaction exists between γ-CD-MOF and CA matrix, also verified by FTIR graphs. No additional peaks appeared after fabrication of CA/γ-CD-MOF hybrid. Therefore, due to pressure gradient gases can permeate through CA/γ-CD-MOF membrane.

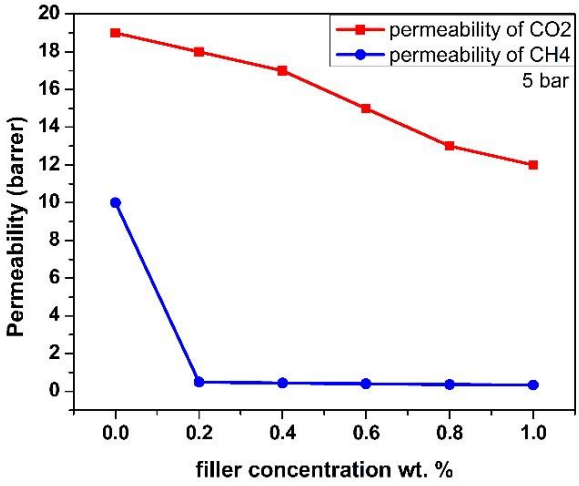

Figure 36: Trend of CO_2/CH_4 permeability with γ-CD-MOF wt.%

4.6.3.2 Effect of feed pressure on gas permeability

The permeability of CO_2 and CH_4 with pressure (1-5) bar in pure cellulose acetate and CA/γ-CD-MOF MMM is presented by graph in figure 37 (a) and (b) and in 38 (a) and (b). In case of pure CA membrane permeability of CO_2 and CH_4 at 1 bar pressure is 30.09 and 15 barrer respectively. With increasing pressure permeability drop from 30.09 to 19 barrer of CO_2 in pristine CA membrane from 1 to 5 bar pressure and slightly increase in selectivity of CO_2/CH_4 observed. Similarly, with the incorporation of filler with different weight percentages (0.2-1 wt. %) in CA overall drop in permeability observed of both CO_2

and CH_4 and significant increase in selectivity appeared of CO_2/CH_4. The reduction in permeability in CA and CA/γ-CD-MOF MMM with increasing pressure is best explain by dual-sorption model. According to this model sorption of gases through polymeric membrane below their glass transition temperature is due to the presence of free volume and excess free volume in glassy polymers. This model comprises of Henry's equation and Langmuir's equation. I.e.

$$C = K_D P + \frac{C_H bp}{1+bp}$$

Where,

K_D is Henry's Law coefficient

$C`_H$ is Langmuir capacity term

b is an affinity parameter[139]

As CA is glassy in nature[140] so it has excess free volume because of orientation of chains and this excess free volume is responsible for the sorption of gas molecule. Koros formulated an equation for the permeability of gases through glassy polymers.

$$P = K_D D_D + \frac{C` bD_H}{1+bP_2}$$

Where,

D_D diffusion coefficient related to Henry's law

D_H diffusion coefficient related to Langmuir law

P_2 is upstream pressure for permeating gas[141]

As in CA/γ-CD-MOF MMM with increasing feed pressure the membrane resists plasticization in its matrix. Hence, with increasing pressure permeability decrease of both CO_2 and CH_4. In case of CH_4 its diffusion rate through polymeric chain is significantly low as compared to CO_2 because of less affinity with Langmuir sorption sites. Therefore, by increasing pressure and simultaneously increasing filler weight percentage in polymeric matrix separation completely achieved because of affinity of permeant gas with

the incorporating group in both polymer and filler. So CO_2 permeate through CA/γ-CD-MOF MMM more preferentially as compared to methane[104].

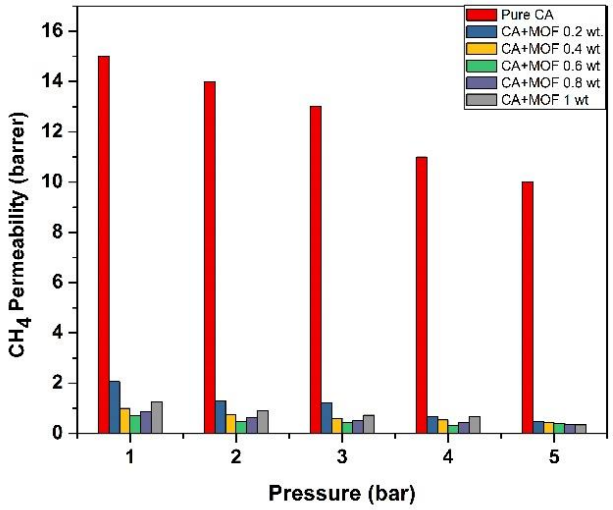

Figure 37: trend of pressure on CH_4 permeability bar graph

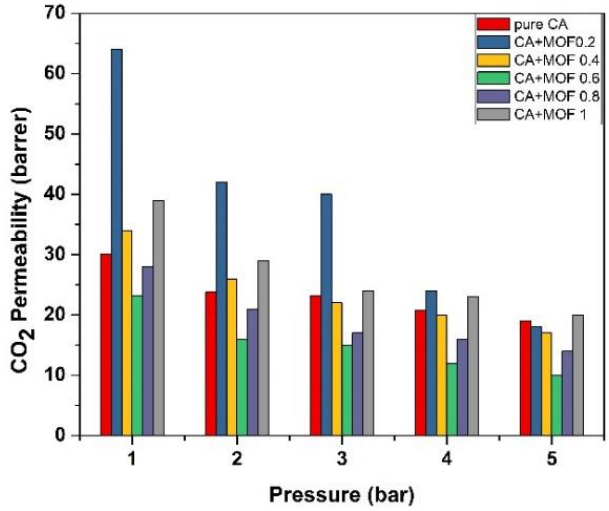

Figure 38: trend of pressure on CO_2 permeability bar graph

4.6.3.3 Effect of feed pressure on of CO_2/CH_4 selectivity

Effect of pressure on the selectivity of CO_2/CH_4 with pressure (1-5 bar) is presented by graph in following figure 39. As shown in bar graph selectivity of CO_2/CH_4 in pristine CA membrane remain below 2.5 in all pressure ranges. In successive membrane sample

of CA/γ-CD-MOF MMM with incorporation of filler selectivity increase considerably. And most optimum value of CO_2/CH_4 selectivity achieved in CA/γ-CD-MOF 0.4 wt. % sample at all pressure ranges (1-5 bar). SEM was employed to observe the surface morphology of pure CA membrane and CA/γ-CD-MOF MMM as shown in figure 39. Figure 39 shows smooth and uniform morphology of pure CA membrane without any voids or cavities over its surface. When γ-CD-MOF incorporated into CA matrix with weight percentage from 0.2% to 1%. With low weight percentage of filler in polymeric matrix, it disperse uniformly over the surface of CA surface without any agglomeration. CA/γ-CD-MOF MMM fabricate with optimum weight percentage of filler is with 1 wt. %. After increasing filler concentration from 1wt. % resulted in the agglomeration of filler on CA surface. This is due to poor dispersion of filler and also due to developmental of van-dar wall forces between filler molecule. It is predicted from FTIR curve and permeation results that γ-CD-MOF incorporated into the free volume exist between the polymeric chain of CA and developed temporary interaction between the hydroxyl group present on its cavities and with hydroxyl group of CA. The increase in selectivity of CO_2/CH_4 is on the basis of affinity of CO_2 with the –OH group presents in large number in both CA and γ-CD-MOF. And in contrast no functional group available that develop affinity towards with methane and having large kinematic diameter of 3.80 Angstrom it finds difficulty in permeating through cavities of γ-CD-MOF as well. So, high value of selectivity 36.79, 38.49, 37, 36 and 35 achieved in CA/γ-CD-MOF 0.2 wt. %, CA/γ-CD-MOF 0.4 wt. %, CA/γ-CD-MOF 0.6 wt. %, CA/γ-CD-MOF 0.8 wt. % and CA/γ-CD-MOF 1 wt. % respectively.

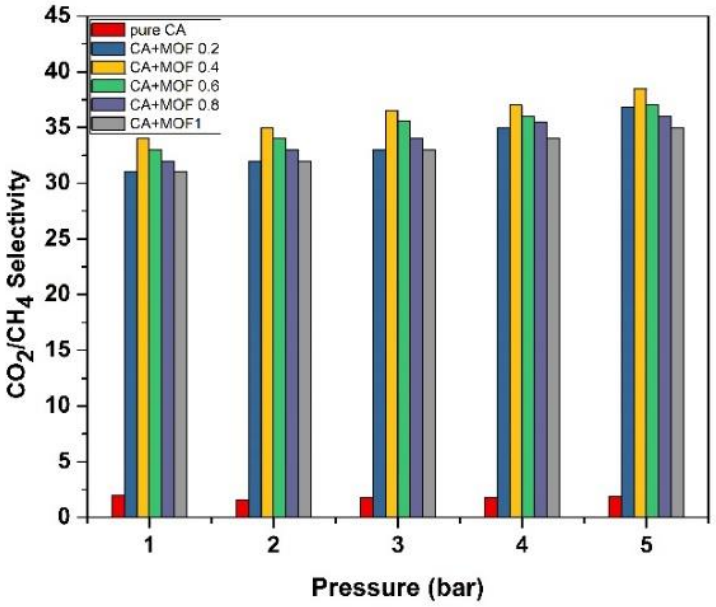

Figure 39: trend of pressure on CO_2/CH_4 Selectivity

4.6.4 Gas permeation results of pure CA and CA/γ-CD-MOF MMM in mixed gas testing

For mixed gas permeation testing, we used CO_2/CH_4 mixture (50:50 by volume). Moreover, we used GC column for checking the composition of the mixture coming out of permeate of the membrane, and this will give us the selectivity of the pure CA and CA/γ-CD-MOF mixed matrix membrane. The values for the gas permeability and the mixed gas selectivity can be shown in the tables 11.

Table 11: Permeation data for pure CA and CA/γ-CD-MOF in mixed gas testing

Membrane	**Permeability CO_2 barrer**	**Permeability CH_4 barrer**	**Selectivity CO_2/CH_4**	**Pressure bar**
Pure CA	26.79	15.04	1.78	1
Pure CA	21.14	14.84	1.42	2
Pure CA	20.60	13.00	1.59	3
Pure CA	18.47	11.52	1.60	4
Pure CA	16.92	10.00	1.69	5
CA+MOF 0.2 wt.%	56.98	2.06	27.61	1
CA+MOF 0.2 wt.%	37.39	1.31	28.50	2
CA+MOF 0.2 wt.%	35.61	1.21	29.39	3
CA+MOF 0.2 wt.%	21.37	0.69	31.17	4
CA+MOF 0.2 wt.%	16.03	0.49	32.77	5

CA+MOF 0.4 wt.%	31.65	0.97	32.67	1
CA+MOF 0.4 wt.%	24.21	0.72	33.64	2
CA+MOF 0.4 wt.%	20.48	0.58	35.08	3
CA+MOF 0.4 wt.%	18.62	0.52	35.56	4
CA+MOF 0.4 wt.%	15.83	0.43	36.99	5
CA+MOF 0.6 wt.%	21.54	0.68	31.71	1
CA+MOF 0.6 wt.%	14.90	0.46	32.67	2
CA+MOF 0.6 wt.%	13.97	0.41	34.16	3
CA+MOF 0.6 wt.%	11.17	0.32	34.60	4
CA+MOF 0.6 wt.%	13.97	0.39	35.56	5
CA+MOF 0.8 wt.%	26.07	0.85	30.75	1
CA+MOF 0.8 wt.%	19.55	0.62	31.71	2
CA+MOF 0.8 wt.%	15.83	0.48	32.67	3
CA+MOF 0.8 wt.%	14.90	0.44	34.12	4
CA+MOF 0.8 wt.%	12.10	0.35	34.60	5
CA+MOF 1 wt.%	36.31	1.22	29.79	1
CA+MOF 1 wt.%	27.00	0.88	30.75	2
CA+MOF 1 wt.%	22.34	0.70	31.71	3
CA+MOF 1 wt.%	21.41	0.66	32.67	4
CA+MOF 1 wt.%	11.17	0.33	33.64	5

4.6.4.1 Effect of filler concentration on gas permeability

In case of mixed gas separation of CO_2/CH_4 (50:50) from pure CA and CA/γ-CD-MOF MMM similar results to that of single gas testing achieved. As shown in graph in figure 40 with increasing the concentration of filler in CA matrix gradual decrease in permeability observed for both CO_2 and CH_4. CA s glassy in nature and follow dual-sorption model for permeation of gases. According to this model glassy polymers have two entirely different phases. One phase is dense for the solubility of permeating gas molecule and second phase composed of uniformly distributed cavities or voids at molecular level. Solute molecules that dissolved in former phase followed Henry's Law and where solute molecules adsorbed on walls of cavities or voids followed Langmuir isotherm. Total solubility of permeating gas molecule is sum of dissolved and adsorbed concentration.

$C_i = C_{Di} + C_{Hi}$

$K_{Di}\ P_i + \frac{C'_H b_i p_i}{1+\sum_j \quad b_j p_j}$

Where, i represent the gas component

K_D Henry's law constant

p_i partial pressure of the dissolving gas

Parameter b characterize the affinity of solute with the walls of adsorbed cavities

C'_H Langmuir adsorption capacity

In this case γ-CD-MOF most probably distribute into free volume available due to glassy nature of polymer. With the increase in concentration of filler more and more available free volume get saturated, hence result in reduction in permeability of gas molecules. Methane having kinematic diameter greater than CO_2 showed very less permeability and drop in permeability for CO_2 also observed[142].

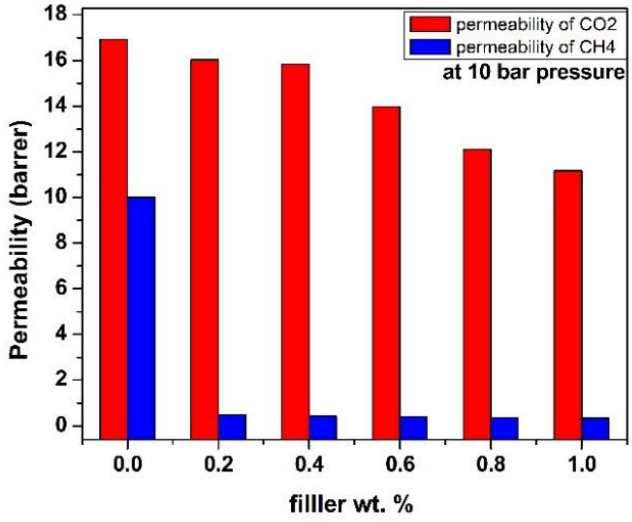

Figure 40: trend of filler wt. % on CO_2 and CH_4 permeability

4.6.4.2 Effect of feed pressure on gas permeability

Permeability of CO_2 and CH_4 in pure CA and CA/γ-CD-MOF membrane samples is shown in figure 41 for CO_2 and in figure 42 for CH_4 plotted against pressure in linear and

bar graph. With marginally drop in permeability's value as compared to single gas testing almost similar trend to that of former gas testing achieved[120].

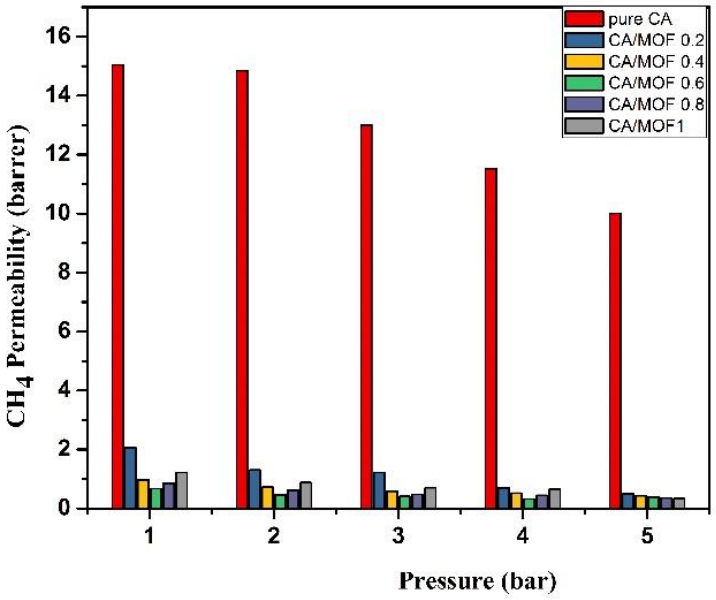

Figure 41: trend of pressure on CH4 permeability

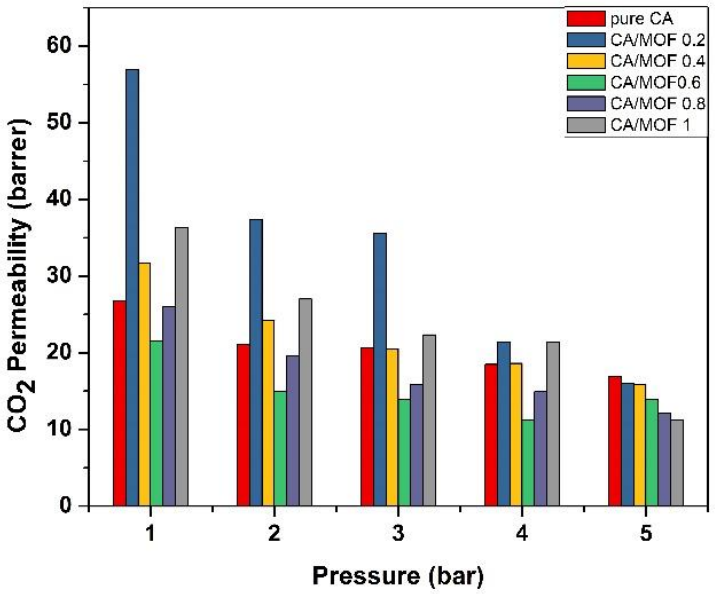

Figure 42: Effect of pressure on permeability of CO_2 in bar graph

4.6.4.3 Effect of feed pressure on the CO_2/CH_4 selectivity

Graph for the increase in feed pressure on the CO_2/CH_4 selectivity is presented in figure 43. With rise in pressure from 1-5 bar considerable increase in selectivity of CO_2/CH_4 observed. When simultaneously both carbon dioxide and methane allowed to pass through CA/γ-CD-MOF MMMM, CO_2 permeates more preferentially as compared to methane. This is because of attached hydroxyl group (-OH) on γ-CD-MOF and CA matrix. These –OH group have affinity towards carbon dioxide and aid it to pass through CA/γ-CD-MOF membrane. In contrast, methane have less affinity with attached functional group so it permeates less. More ever due to large kinematic diameter 3.8 Angstrom it cannot permeate through Langmuir sorption sites[142].

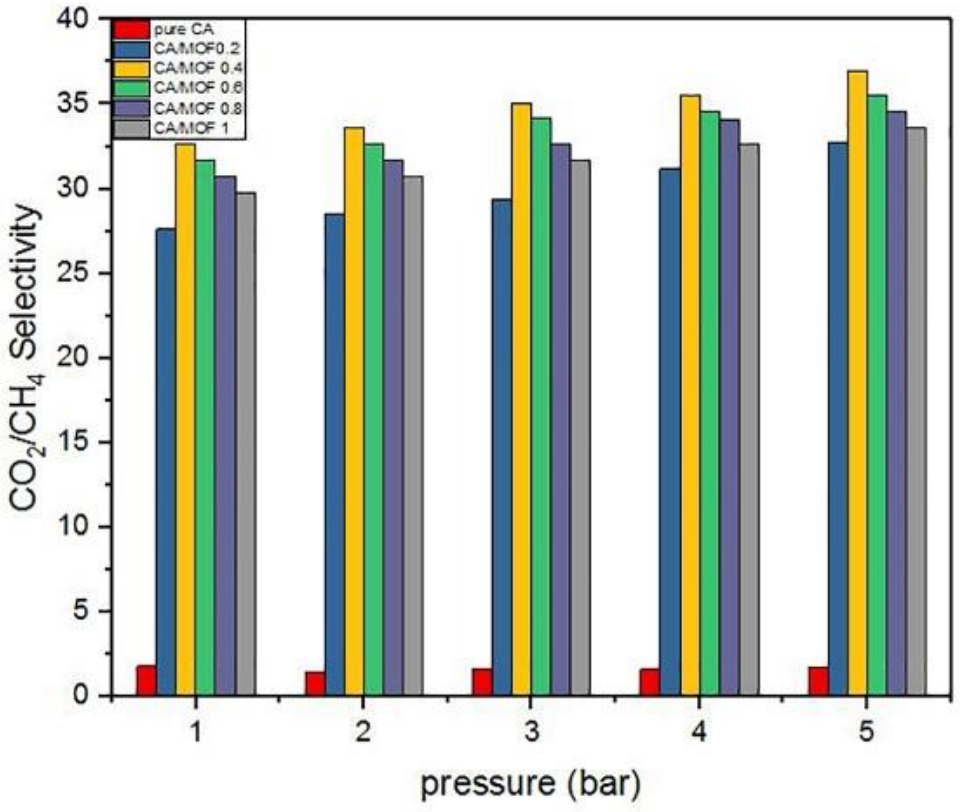

Figure 43: trend of pressure on selectivity of CO_2/CH_4 with pressure

Conclusion

This thesis comprises of the fabrication of membranes by incorporating γ-CD-MOF into in two different polymers i.e. CA and PU and synthesized CA/γ-CD-MOF and PU/γ-CD-MOF MMM. Weight percentage of both polymers and filler were optimized for membrane fabrication and trends in permeability and selectivity were measured precisely. Mixed matrix membrane from CA and PU were undergo single and mixed gas permeation testing and best samples on the basis of permeability and selectivity were analyzed. These samples were characterized using SEM, FTIR, XRD and ultimate tensile strength analysis. FTIR spectroscopy was carried out to check the availability of the required functional groups. SEM analysis was done to study the morphology, surface properties and cross-sections of the synthesized membranes. XRD analysis was done to examine the percentage of crystallinity in polymer and in filler after being incorporated into the polymeric matrix. Finally, tensile testing was carried out to check the mechanical integrity of the membrane samples. After careful characterization technique analysis and single and mixed gas permeation testing of both CA/γ-CD-MOF and PU/γ-CD-MOF MMM were done and very appealing results were obtained. PU/γ-CD-MOF MMM offer higher permeability of CO_2 as well as good CO_2/CH_4 selectivity in range of 25-29. In addition, PU/γ-CD-MOF membrane is hydrophobic in nature and provide sufficient resistance from being swelling from moisture content in feed. These peculiar characteristics are due to dense hydrophobic nature of PU and also provide homogeneous medium for the distribution of filler. Furthermore, PU have semi-crystalline nature in the form of soft and hard segments, and it gives PU/γ-CD-MOF membrane a high strain rate and PU/γ-CD-MOF 0.6 wt.% can bear the maximum tensile stress up to 24 MPA. Although physical interaction exist between PU and γ-Cd-MOF in PU/γ-CD-MOF MMM and verified by FTIR, because no additional peaks were appeared before and after making the hybrid.

Secondly CA/γ-CD-MOF MMM were classified under hydrophilic membrane category. Because both CA and filler lose their innate characteristics on encounter with moisture. While, CA/γ-CD-MOF membrane shows higher CO_2/CH_4 selectivity up to 39. However, optimum permeability of CO_2 achieved in CA/γ-CD-MOF 0.4 wt. % is 17 barrer and CO_2/CH_4 selectivity of 38.49. Similar to PU/γ-CD-MOF membrane interaction between CA and γ-Cd-mof is also of physical nature and confirmed by FTIR graph. In both

polymer with increased in filler loading above 1 wt. % poor dispersion of filler appeared. So 1wt. % is the optimum concentration of filler in polymer matrix.

Finally either to achieve optimum CO_2/CH_4 selectivity and maintain sustainable resistance against swelling due to moisture content then PU/γ-Cd-mof is the best candidate. On contrary just to achieve high CO_2/CH_4 selectivity with better mechanical strength then CA/γ-CD-mof should be given preference.

Table 12: comparison of PU mixed matrix membrane with this study

Membrane	Permeability of CO_2 barrer	Permeability of CH_4	$\alpha CO_2/CH_4$	Reference
PU-Al_2O_3	78.28	3.95	19.82	[102]
PU-ZnO	55	3.81	14.43	[143]
PU-EP20	134	8.2	16.4	[144]
PU/silica nano-particle			23.4	[129]
PU/silica	120	8.93	13.43	[131]
PU/γ-CD-MOF 0.2 wt.%	214	7.49	28.56	This study
PU/γ-CD-MOF 0.4 wt.%	195	8.6	22.48	This study

Table 13: comparison of CA mixed matrix membrane with this study

Membrane	Permeability of CO_2 barrer	Permeability of CH_4	$\alpha CO_2/CH_4$	Reference
CA/PEG (10%)	19.31	0.489	39.47	[128]
CA/Tf_2N	8.9	0.4	22.25	[145]
CA/NH_2-MIL-53(Al)	52.6	1.8	29.22	[146]
CA/γ-CD-MOF 0.2 wt.%	18	0.489	36.79	This study
CA/γ-CD-MOF 0.4 wt.%	17	0.441	38.49	This study
CA/γ-CD-MOF 0. 6 wt.%	15	0.405	37	This study
CA/γ-CD-MOF 0.8 wt.%	13	0.361	36	This study

On the basis of above findings and results obtained from polyurethane and cellulose acetate mixed matrix membrane it is recommended that in future following are the areas which should be addressed:

- Synthesize composite membrane to enhance permeability of carbon dioxide and optimize selectivity.
- Durability of membranes should be tested for longer period of time against pressure, plasticizing and swelling resistance.
- Simultaneously focus should be given on the utilization of new polymers i.e. polymeric intrinsic microporosty PIM, 6FDA-DABA, PDMS etc. because literature narrates the significant increase in permeability and selectivity in CO_2, CH_4, N_2 and O_2 from membrane fabricated from these polymers.

References

[1] Now, C., *Earth's CO2 home page*. 2015.

[2] Othman, M., et al., *Separability of carbon dioxide from methane using MFI zeolite–silica film deposited on gamma-alumina support.* 2009. **121**(1-3): p. 138-144.

[3] Yang, H., et al., *Progress in carbon dioxide separation and capture: A review.* 2008. **20**(1): p. 14-27.

[4] Baldus, W., D.J.M.i.G.S. Tillman, and Enrichment, *Conditions which need to be fulfilled by membrane systems in order to compete with existing methods for gas separation.* 1986: p. 2642.

[5] Bernardo, P., E. Drioli, and G. Golemme, *Membrane Gas Separation: A Review/State of the Art.* Industrial & Engineering Chemistry Research, 2009. **48**(10): p. 4638-4663.

[6] Freeman, B.D., *Basis of Permeability/Selectivity Tradeoff Relations in Polymeric Gas Separation Membranes.* Macromolecules, 1999. **32**(2): p. 375-380.

[7] Robeson, L.M., *Correlation of separation factor versus permeability for polymeric membranes.* Journal of Membrane Science, 1991. **62**(2): p. 165-185.

[8] Aoki, T., *Macromolecular design of permselective membranes.* Progress in Polymer Science, 1999. **24**(7): p. 951-993.

[9] Galizia, M., et al., *50th Anniversary Perspective: Polymers and Mixed Matrix Membranes for Gas and Vapor Separation: A Review and Prospective Opportunities.* Macromolecules, 2017. **50**(20): p. 7809-7843.

[10] Javaid, A.J.C.E.J., *Membranes for solubility-based gas separation applications.* 2005. **112**(1-3): p. 219-226.

[11] Budd, P.M. and N.B.J.P.C. McKeown, *Highly permeable polymers for gas separation membranes.* 2010. **1**(1): p. 63-68.

[12] Hofmann, D., E.J.M.O.i.s. Tocci, and transformations, *Molecular modeling, A tool for the knowledge-based design of polymer-based membrane materials.* 2009: p. 3-18.

[13] Park, H.B., et al., *Thermally rearranged (TR) polymer membranes for CO2 separation.* 2010. **359**(1-2): p. 11-24.

[14] Wind, J.D., D.R. Paul, and W.J.J.J.o.M.S. Koros, *Natural gas permeation in polyimide membranes.* 2004. **228**(2): p. 227-236.

[15] Deng, L., T.-J. Kim, and M.-B.J.J.o.M.S. Hägg, *Facilitated transport of CO2 in novel PVAm/PVA blend membrane.* 2009. **340**(1-2): p. 154-163.

[16] Barlow, J., D.J.P.E. Paul, and Science, *Polymer blends and alloys—a review of selected considerations.* 1981. **21**(15): p. 985-996.

[17] Wang, D., K. Li, and W.J.J.o.M.S. Teo, *Polyethersulfone hollow fiber gas separation membranes prepared from NMP/alcohol solvent systems.* 1996. **115**(1): p. 85-108.

[18] Panapitiya, N., et al., *Compatibilized immiscible polymer blends for gas separations.* 2016. **9**(8): p. 643.

[19] Galizia, M., et al., *50th anniversary perspective: Polymers and mixed matrix membranes for gas and vapor separation: A review and prospective opportunities.* 2017. **50**(20): p. 7809-7843.

[20] Vu, D.Q., W.J. Koros, and S.J.J.J.o.M.S. Miller, *Mixed matrix membranes using carbon molecular sieves: I. Preparation and experimental results.* 2003. **211**(2): p. 311-334.

[21] Zornoza, B., et al., *Metal organic framework based mixed matrix membranes: An increasingly important field of research with a large application potential.* 2013. **166**: p. 67-78.

[22] Barrer, R.M.J.Z., *Zeolites and their synthesis.* 1981. **1**(3): p. 130-140.

[23] Mahajan, R., W.J.J.P.E. Koros, and Science, *Mixed matrix membrane materials with glassy polymers. Part 1.* 2002. **42**(7): p. 1420-1431.

[24] Dahe, G.J., R.S. Teotia, and J.R.J.C.e.j. Bellare, *The role of zeolite nanoparticles additive on morphology, mechanical properties and performance of polysulfone hollow fiber membranes.* 2012. **197**: p. 398-406.

[25] Batten, S.R., et al., *Terminology of metal–organic frameworks and coordination polymers (IUPAC Recommendations 2013).* 2013. **85**(8): p. 1715-1724.

[26] Li, H., et al., *Design and synthesis of an exceptionally stable and highly porous metal-organic framework.* 1999. **402**(6759): p. 276.

[27] Chui, S.S.-Y., et al., *A chemically functionalizable nanoporous material [Cu3 (TMA) 2 (H2O) 3] n.* 1999. **283**(5405): p. 1148-1150.

[28] Hoskins, B. and R.J.J.o.t.A.C.S. Robson, *Design and construction of a new class of scaffolding-like materials comprising infinite polymeric frameworks of 3D-linked molecular rods. A reappraisal of the zinc cyanide and cadmium cyanide structures and the synthesis and structure of the diamond-related frameworks [N (CH3) 4][CuIZnII (CN) 4] and CuI [4, 4', 4'', 4'''-tetracyanotetraphenylmethane] BF4. xC6H5NO2.* 1990. **112**(4): p. 1546-1554.

[29] Yaghi, O. and H.J.J.o.t.A.C.S. Li, *Hydrothermal synthesis of a metal-organic framework containing large rectangular channels.* 1995. **117**(41): p. 10401-10402.

[30] Yaghi, O.M., G. Li, and H.J.N. Li, *Selective binding and removal of guests in a microporous metal–organic framework.* 1995. **378**(6558): p. 703.

[31] Furukawa, H., et al., *The chemistry and applications of metal-organic frameworks.* 2013. **341**(6149): p. 1230444.

[32] Cui, J., et al., *Photonic metal–organic framework composite spheres: a new kind of optical material with self-reporting molecular recognition.* 2014. **6**(20): p. 11995-12001.

[33] Kumar, P., et al., *Luminescent nanocrystal metal organic framework based biosensor for molecular recognition.* 2014. **43**: p. 114-117.

[34] Kılıç, A., et al., *Sod-ZMOF/Matrimid® mixed matrix membranes for CO2 separation.* 2015. **489**: p. 81-89.

[35] Li, R.-J., et al., *ROD-8, a rod MOF with a pyrene-cored tetracarboxylate linker: framework disorder, derived nets and selective gas adsorption.* CrystEngComm, 2014. **16**(28): p. 6291-6295.

[36] Kumar, A. and S.J.J.o.D.R. Maskara, *Revealing clinicians' experiences towards healthcare software usability using human–centred design approach.* 2015. **13**(1): p. 36-54.

[37] Miller, S.R., et al., *Biodegradable therapeutic MOFs for the delivery of bioactive molecules.* Chemical Communications, 2010. **46**(25): p. 4526-4528.

[38] Al-Janabi, N., et al., *Mapping the Cu-BTC metal–organic framework (HKUST-1) stability envelope in the presence of water vapour for CO2 adsorption from flue gases.* 2015. **281**: p. 669-677.

[39] Sorribas, S., et al., *Pervaporation and membrane reactor performance of polyimide based mixed matrix membranes containing MOF HKUST-1.* 2015. **124**: p. 37-44.

[40] Kim, H.K., et al., *A Chemical route to activation of open metal sites in the copper-based metal–organic framework materials HKUST-1 and Cu-MOF-2.* 2015. **137**(31): p. 10009-10015.

[41] Basu, S., A. Cano-Odena, and I.F.J.J.o.m.s. Vankelecom, *Asymmetric Matrimid®/[Cu3 (BTC) 2] mixed-matrix membranes for gas separations.* 2010. **362**(1-2): p. 478-487.

[42] Lin, R., et al., *Ionic liquids as the MOFs/polymer interfacial binder for efficient membrane separation.* 2016. **8**(46): p. 32041-32049.

[43] Nakagaki, S., et al., *Chemical reactions catalyzed by metalloporphyrin-based metal-organic frameworks.* 2013. **18**(6): p. 7279-7308.

[44] Park, K.S., et al., *Exceptional chemical and thermal stability of zeolitic imidazolate frameworks.* 2006. **103**(27): p. 10186-10191.

[45] Casco, M.E., et al., *Gate-opening effect in ZIF-8: the first experimental proof using inelastic neutron scattering.* 2016. **52**(18): p. 3639-3642.

[46] Zhang, K., et al., *Exploring the framework hydrophobicity and flexibility of ZIF-8: from biofuel recovery to hydrocarbon separations.* 2013. **4**(21): p. 3618-3622.

[47] Zhang, C., et al., *High performance ZIF-8/6FDA-DAM mixed matrix membrane for propylene/propane separations.* 2012. **389**: p. 34-42.

[48] Lee, Y.-R., et al., *ZIF-8: A comparison of synthesis methods.* Chemical Engineering Journal, 2015. **271**: p. 276-280.

[49] Boutin, A., et al., *The behavior of flexible MIL-53 (Al) upon CH4 and CO2 adsorption.* 2010. **114**(50): p. 22237-22244.

[50] Bourrelly, S., et al., *Explanation of the adsorption of polar vapors in the highly flexible metal organic framework MIL-53 (Cr).* 2010. **132**(27): p. 9488-9498.

[51] Llewellyn, P., et al., *Complex adsorption of short linear alkanes in the flexible metal-organic-framework MIL-53 (Fe).* 2009. **131**(36): p. 13002-13008.

[52] Serre, C., et al., *Very Large Breathing Effect in the First Nanoporous Chromium (III)-Based Solids: MIL-53 or CrIII (OH)⊙{O2C− C6H4− CO2}⊙{HO2C− C6H4− CO2H} x⊙ H2O y.* 2002. **124**(45): p. 13519-13526.

[53] Loiseau, T., et al., *A rationale for the large breathing of the porous aluminum terephthalate (MIL-53) upon hydration.* 2004. **10**(6): p. 1373-1382.

[54] Sabetghadam, A., et al., *Metal Organic Framework Crystals in Mixed-Matrix Membranes: Impact of the Filler Morphology on the Gas Separation Performance.* 2016. **26**(18): p. 3154-3163.

[55] Rosi, N.L., et al., *Rod packings and metal− organic frameworks constructed from rod-shaped secondary building units.* 2005. **127**(5): p. 1504-1518.

[56] Millward, A.R. and O.M.J.J.o.t.A.C.S. Yaghi, *Metal− organic frameworks with exceptionally high capacity for storage of carbon dioxide at room temperature.* 2005. **127**(51): p. 17998-17999.

[57] Britt, D., et al., *Highly efficient separation of carbon dioxide by a metal-organic framework replete with open metal sites.* 2009. **106**(49): p. 20637-20640.

[58] Bachman, J.E., et al., *Enhanced ethylene separation and plasticization resistance in polymer membranes incorporating metal–organic framework nanocrystals.* 2016. **15**(8): p. 845.

[59] Zhang, L., et al., *Coumarin-modified microporous-mesoporous Zn-MOF-74 showing ultra-high uptake capacity and photo-switched storage/release of UVI ions.* 2016. **311**: p. 30-36.

[60] Forgan, R.S., et al., *Nanoporous Carbohydrate Metal–Organic Frameworks.* Journal of the American Chemical Society, 2012. **134**(1): p. 406-417.

[61] Furukawa, Y., et al., *Nano-and Microsized Cubic Gel Particles from Cyclodextrin Metal–Organic Frameworks.* 2012. **124**(42): p. 10718-10721.

[62] Smaldone, R.A., et al., *Metal–organic frameworks from edible natural products.* 2010. **49**(46): p. 8630-8634.

[63] Gassensmith, J.J., et al., *Strong and reversible binding of carbon dioxide in a green metal–organic framework.* 2011. **133**(39): p. 15312-15315.

[64] Smith, M.K., S.R. Angle, and B.H. Northrop, *Preparation and Analysis of Cyclodextrin-Based Metal–Organic Frameworks: Laboratory Experiments Adaptable for High School through Advanced Undergraduate Students.* Journal of Chemical Education, 2015. **92**(2): p. 368-372.

[65] Mischnick, P. and D. Momcilovic, *Chemical structure analysis of starch and cellulose derivatives*, in *Advances in carbohydrate chemistry and biochemistry*. 2010, Elsevier. p. 117-210.

[66] Abedini, R., S.M. Mousavi, and R.J.D. Aminzadeh, *A novel cellulose acetate (CA) membrane using TiO2 nanoparticles: preparation, characterization and permeation study.* 2011. **277**(1-3): p. 40-45.

[67] Galland, G. and T.J.J.o.a.p.s. Lam, *Permeability and diffusion of gases in segmented polyurethanes: structure–properties relations.* 1993. **50**(6): p. 1041-1058.

[68] Eddaoudi, M., et al., *Systematic design of pore size and functionality in isoreticular MOFs and their application in methane storage.* 2002. **295**(5554): p. 469-472.

[69] Li, J.-R., R.J. Kuppler, and H.-C.J.C.S.R. Zhou, *Selective gas adsorption and separation in metal–organic frameworks.* 2009. **38**(5): p. 1477-1504.

[70] Li, J.-R., J. Sculley, and H.-C.J.C.r. Zhou, *Metal–organic frameworks for separations.* 2011. **112**(2): p. 869-932.

[71] Nugent, P., et al., *Porous materials with optimal adsorption thermodynamics and kinetics for CO 2 separation.* 2013. **495**(7439): p. 80.

[72] Eddaoudi, M., H. Li, and O.J.J.o.t.A.C.S. Yaghi, *Highly porous and stable metal− organic frameworks: structure design and sorption properties.* 2000. **122**(7): p. 1391-1397.

[73] Cavka, J.H., et al., *A new zirconium inorganic building brick forming metal organic frameworks with exceptional stability.* 2008. **130**(42): p. 13850-13851.

[74] Garibay, S.J. and S.M.J.C.c. Cohen, *Isoreticular synthesis and modification of frameworks with the UiO-66 topology.* 2010. **46**(41): p. 7700-7702.

[75] Lin, X., et al., *High capacity hydrogen adsorption in Cu (II) tetracarboxylate framework materials: the role of pore size, ligand functionalization, and exposed metal sites.* 2009. **131**(6): p. 2159-2171.

[76] Wang, B., et al., *Applications of metal-organic frameworks for green energy and environment: New advances in adsorptive gas separation, storage and removal.* 2018.

[77] Chen, K.-J., et al., *Tuning Pore Size in Square-Lattice Coordination Networks for Size-Selective Sieving of CO2.* 2016. **55**(35): p. 10268-10272.

[78] Bao, S.-J., et al., *A stable metal–organic framework with suitable pore sizes and rich uncoordinated nitrogen atoms on the internal surface of micropores for highly efficient CO 2 capture.* 2015. **3**(14): p. 7361-7367.

[79] Xiang, S., et al., *Microporous metal-organic framework with potential for carbon dioxide capture at ambient conditions.* 2012. **3**: p. 954.

[80] Wang, R., et al., *A Zn metal–organic framework with high stability and sorption selectivity for CO2.* 2015. **54**(22): p. 10587-10592.

[81] Lin, Y., et al., *Polyethyleneimine incorporated metal-organic frameworks adsorbent for highly selective CO 2 capture.* 2013. **3**: p. 1859.

[82] Furukawa, H., et al., *Ultrahigh porosity in metal-organic frameworks.* 2010. **329**(5990): p. 424-428.

[83] Farha, O.K., et al., *De novo synthesis of a metal–organic framework material featuring ultrahigh surface area and gas storage capacities.* 2010. **2**(11): p. 944.

[84] Moellmer, J., et al., *High pressure adsorption of hydrogen, nitrogen, carbon dioxide and methane on the metal–organic framework HKUST-1.* 2011. **138**(1-3): p. 140-148.

[85] Yazaydın, A.O.z.r., et al., *Screening of metal− organic frameworks for carbon dioxide capture from flue gas using a combined experimental and modeling approach.* 2009. **131**(51): p. 18198-18199.

[86] Saha, D., et al., *Adsorption of CO2, CH4, N2O, and N2 on MOF-5, MOF-177, and zeolite 5A.* 2010. **44**(5): p. 1820-1826.

[87] Chowdhury, P., C. Bikkina, and S.J.T.J.o.P.C.C. Gumma, *Gas adsorption properties of the chromium-based metal organic framework MIL-101.* 2009. **113**(16): p. 6616-6621.

[88] Villiers, A.J.C.R., *Discovery of cyclodextrins.* 1891. **112**: p. 536.

[89] Stella, V.J. and R.A.J.P.r. Rajewski, *Cyclodextrins: their future in drug formulation and delivery.* 1997. **14**(5): p. 556-567.

[90] Matsuda, H. and H.J.A.d.d.r. Arima, *Cyclodextrins in transdermal and rectal delivery.* 1999. **36**(1): p. 81-99.

[91] Mabuchi, N. and M.J.J.P.J. Ngoa, *Controlled release powdered flavour preparations and confectioneries containing preparations.* 2001. **128**: p. 638.

[92] Hirose, T. and Y.J.J.P.J. Yamamoto, *Hinokitol containing cyclo-olefin polymer compositions and their molding with excellent antimicrobial and gas barrier properties.* 2001. **55480**.

[93] Del Valle, E.M.J.P.b., *Cyclodextrins and their uses: a review.* 2004. **39**(9): p. 1033-1046.

[94] Liu, B., et al., *Optimized synthesis and crystalline stability of γ-cyclodextrin metal-organic frameworks for drug adsorption.* 2016. **514**(1): p. 212-219.

[95] Hartlieb, K.J., et al., *CD-MOF: A versatile separation medium.* 2016. **138**(7): p. 2292-2301.

[96] Lee, K.B., et al., *Chemisorption of carbon dioxide on sodium oxide promoted alumina.* 2007. **53**(11): p. 2824-2831.

[97] Jin, Y., et al., *A shape-persistent organic molecular cage with high selectivity for the adsorption of CO2 over N2.* 2010. **122**(36): p. 6492-6495.

[98] Forgan, R.S., et al., *Nanoporous carbohydrate metal–organic frameworks.* 2011. **134**(1): p. 406-417.

[99] Ghalei, B., et al., *Polyurethane-mesoporous silica gas separation membranes.* 2018. **29**(2): p. 874-883.

[100] Soltani, B. and M.J.M. Asghari, *Effects of ZnO nanoparticle on the gas separation performance of polyurethane mixed matrix membrane.* 2017. **7**(3): p. 43.

[101] Amedi, H.R., M.J.J.o.N.G.S. Aghajani, and Engineering, *Gas separation in mixed matrix membranes based on polyurethane containing SiO2, ZSM-5, and ZIF-8 nanoparticles.* 2016. **35**: p. 695-702.

[102] Ameri, E., et al., *Enhancement of the gas separation properties of polyurethane membranes by alumina nanoparticles.* Journal of Membrane Science, 2015. **479**: p. 11-19.

[103] Isfahani, A.P., et al., *Enhancement of the gas separation properties of polyurethane membrane by epoxy nanoparticles.* Journal of Industrial and Engineering Chemistry, 2016. **44**: p. 67-72.

[104] Sanaeepur, H., B. Nasernejad, and A. Kargari, *Cellulose acetate/nano-porous zeolite mixed matrix membrane for CO2 separation.* 2015. **5**(3): p. 291-304.

[105] Hussain, A., et al., *Carbon capture from natural gas using multi-walled CNTs based mixed matrix membranes.* 2017: p. 1-12.

[106] Farrukh, S., et al., *Blending of TiO2 nanoparticles with cellulose acetate polymer: to study the effect on morphology and gas permeation of blended membranes.* 2014. **9**(4): p. 543-551.

[107] Moghadassi, A.R., et al., *Fabrication and modification of cellulose acetate based mixed matrix membrane: Gas separation and physical properties.* Journal of Industrial and Engineering Chemistry, 2014. **20**(3): p. 1050-1060.

[108] Mubashir, M., et al., *Efficient CO 2 /N 2 and CO 2 /CH 4 separation using NH 2 -MIL-53(Al)/cellulose acetate (CA) mixed matrix membranes*. Vol. 199. 2018.

[109] Ojeda, J. and M. Dittrich, *Fourier Transform Infrared Spectroscopy for Molecular Analysis of Microbial Cells*. Vol. 881. 2012. 187-211.

[110] McCluskey, M., *Local Vibrational Modes of Impurities in Semiconductors*. Vol. 87. 2000. 3593-3617.

[111] Goldstein, J.I., et al., *Scanning electron microscopy and X-ray microanalysis*. 2017: Springer.

[112] SMITH, A.K.J.E.N.A.B.-u.A., *Imaging Nanostucture.* 2014: p. 210.

[113] Gunasekaran, K., P. Kumar, and M. Lakshmipathy, *Mechanical and bond properties of coconut shell concrete*. Vol. 25. 2011. 92-98.

[114] Inaba, K., et al., *High resolution x-ray diffraction analyses of (La, Sr) MnO3/ZnO/sapphire (0001) double heteroepitaxial films.* 2013. **3**(01): p. 72.

[115] Grob, R.L. and E.F. Barry, *Modern practice of gas chromatography*. 2004: John Wiley & Sons.

[116] Yang, Y., et al., *Enhancing the mechanical strength and CO2/CH4 separation performance of polymeric membranes by incorporating amine-appended porous polymers.* 2019. **569**: p. 149-156.

[117] Liu, B., et al., *Optimized synthesis and crystalline stability of gamma-cyclodextrin metal-organic frameworks for drug adsorption.* Int J Pharm, 2016. **514**(1): p. 212-219.

[118] Sanaeepur, H., et al., *A novel Co2+ exchanged zeolite Y/cellulose acetate mixed matrix membrane for CO2/N2 separation.* 2016. **60**: p. 403-413.

[119] Sanaeepur, H., et al., *Cellulose acetate/nano-porous zeolite mixed matrix membrane for CO2 separation.* 2015. **5**(3): p. 291-304.

[120] Ahmad, A.L., et al., *A cellulose acetate/multi-walled carbon nanotube mixed matrix membrane for CO2/N2 separation.* Journal of Membrane Science, 2014. **451**: p. 55-66.

[121] Liu, B., et al., *Microwave-Assisted Rapid Synthesis of γ-Cyclodextrin Metal–Organic Frameworks for Size Control and Efficient Drug Loading.* Crystal Growth & Design, 2017. **17**(4): p. 1654-1660.

[122] Ahmad, A., et al., *A cellulose acetate/multi-walled carbon nanotube mixed matrix membrane for CO2/N2 separation.* 2014. **451**: p. 55-66.

[123] Mubashir, M., et al., *Efficient CO2/N2 and CO2/CH4 separation using NH2-MIL-53 (Al)/cellulose acetate (CA) mixed matrix membranes.* 2018. **199**: p. 140-151.

[124] Mozaffari, V., et al., *Gas separation properties of polyurethane/poly(ether-block-amide) (PU/PEBA) blend membranes.* Separation and Purification Technology, 2017. **185**: p. 202-214.

[125] *Gas transport properties of segmented polyurethanes varying in the kind of soft segments.* Separation and Purification Technology, 2007. **57**(3): p. 413-417.

[126] Talakesh, M.M., et al., *Gas separation properties of poly(ethylene glycol)/poly(tetramethylene glycol) based polyurethane membranes.* Journal of Membrane Science, 2012. **415-416**: p. 469-477.

[127] Sanaeepur, H., A. Kargari, and B. Nasernejad, *Aminosilane-functionalization of a nanoporous Y-type zeolite for application in a cellulose acetate based mixed matrix membrane for CO2 separation.* RSC Advances, 2014. **4**(109): p. 63966-63976.

[128] Hussain, A., et al., *Carbon capture from natural gas using multi-walled CNTs based mixed matrix membranes.* Environmental Technology, 2019. **40**(7): p. 843-854.

[129] Amedi, H. and M. Aghajani, *Gas separation in mixed matrix membranes based on polyurethane containing SiO2, ZSM-5, and ZIF-8 nanoparticles*. Vol. 35. 2016.

[130] Merkel, T.C., et al., *Effect of Nanoparticles on Gas Sorption and Transport in Poly(1-trimethylsilyl-1-propyne).* Macromolecules, 2003. **36**(18): p. 6844-6855.

[131] Sadeghi, M., et al., *Gas separation properties of polyether-based polyurethane–silica nanocomposite membranes.* Journal of Membrane Science, 2011. **376**(1): p. 188-195.

[132] Sadeghi, M., M.A. Semsarzadeh, and H. Moadel, *Enhancement of the gas separation properties of polybenzimidazole (PBI) membrane by incorporation of silica nano particles.* Journal of Membrane Science, 2009. **331**(1): p. 21-30.

[133] Amedi, H.R. and M. Aghajani, *Gas separation in mixed matrix membranes based on polyurethane containing SiO2, ZSM-5, and ZIF-8 nanoparticles.* Journal of Natural Gas Science and Engineering, 2016. **35**: p. 695-702.

[134] Genduso, G., et al., *Mixed-gas sorption in polymers via a new barometric test system: sorption and diffusion of CO2-CH4 mixtures in polydimethylsiloxane (PDMS).* Journal of Membrane Science, 2019. **577**: p. 195-204.

[135] Genduso, G., B.S. Ghanem, and I. Pinnau, *Experimental Mixed-Gas Permeability, Sorption and Diffusion of CO2-CH4 Mixtures in 6FDA-mPDA Polyimide Membrane: Unveiling the Effect of Competitive Sorption on Permeability Selectivity.* 2019. **9**(1): p. 10.

[136] Wijmans, J.G. and R.W. Baker, *The solution-diffusion model: a review.* Journal of Membrane Science, 1995. **107**(1): p. 1-21.

[137] Hassanajili, S., M. Khademi, and P. Keshavarz, *Influence of various types of silica nanoparticles on permeation properties of polyurethane/silica mixed matrix membranes.* Journal of Membrane Science, 2014. **453**: p. 369-383.

[138] Kuznetsova, A., et al., *Physical adsorption of xenon in open single walled carbon nanotubes: Observation of a quasi-one-dimensional confined Xe phase.* 2000. **112**(21): p. 9590-9598.

[139] Horn, N.R. and D.R. Paul, *Carbon Dioxide Sorption and Plasticization of Thin Glassy Polymer Films Tracked by Optical Methods.* Macromolecules, 2012. **45**(6): p. 2820-2834.

[140] Rosenbaum, S. and O. Cotton, *Steady-state distribution of water in cellulose acetate membrane.* 1969. **7**(1): p. 101-109.

[141] Paul, D.R. and W.J. Koros, *Effect of partially immobilizing sorption on permeability and the diffusion time lag.* 1976. **14**(4): p. 675-685.

[142] Donohue, M.D., B.S. Minhas, and S.Y. Lee, *Permeation behavior of carbon dioxide-methane mixtures in cellulose acetate membranes.* Journal of Membrane Science, 1989. **42**(3): p. 197-214.

[143] Soltani, B. and M. Asghari, *Effects of ZnO Nanoparticle on the Gas Separation Performance of Polyurethane Mixed Matrix Membrane.* Membranes (Basel), 2017. **7**(3).

[144] Ameri, E., et al., *Enhancement of the gas separation properties of polyurethane membranes by alumina nanoparticles*. Vol. 479. 2015.

[145] Nikolaeva, D., et al., *The performance of affordable and stable cellulose-based poly-ionic membranes in CO2/N2 and CO2/CH4 gas separation.* Journal of Membrane Science, 2018. **564**: p. 552-561.

[146] Mubashir, M., et al., *Efficient CO2/N2 and CO2/CH4 separation using NH2-MIL-53(Al)/cellulose acetate (CA) mixed matrix membranes.* Separation and Purification Technology, 2018. **199**: p. 140-151.